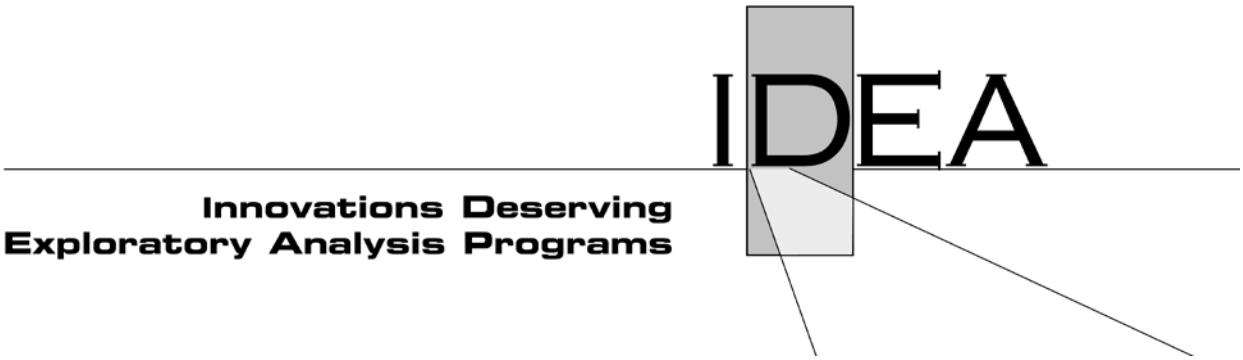

NCHRP IDEA Program

Biomimetic Antifreeze Molecules: A Novel Solution to Deicing Salts and Air-Entraining Admixtures

Final Report for
NCHRP IDEA Project 204

Prepared by:
Wil V. Srubar III, Ph.D.
University of Colorado Boulder

December 2019

TRB TRANSPORTATION RESEARCH BOARD
The National Academies of
SCIENCES · ENGINEERING · MEDICINE

Innovations Deserving Exploratory Analysis (IDEA) Programs Managed by the Transportation Research Board

This IDEA project was funded by the NCHRP IDEA Program.

The TRB currently manages the following three IDEA programs:

- The NCHRP IDEA Program, which focuses on advances in the design, construction, and maintenance of highway systems, is funded by American Association of State Highway and Transportation Officials (AASHTO) as part of the National Cooperative Highway Research Program (NCHRP).
- The Safety IDEA Program currently focuses on innovative approaches for improving railroad safety or performance. The program is currently funded by the Federal Railroad Administration (FRA). The program was previously jointly funded by the Federal Motor Carrier Safety Administration (FMCSA) and the FRA.
- The Transit IDEA Program, which supports development and testing of innovative concepts and methods for advancing transit practice, is funded by the Federal Transit Administration (FTA) as part of the Transit Cooperative Research Program (TCRP).

Management of the three IDEA programs is coordinated to promote the development and testing of innovative concepts, methods, and technologies.

For information on the IDEA programs, check the IDEA website (www.trb.org/idea). For questions, contact the IDEA programs office by telephone at (202) 334-3310.

IDEA Programs
Transportation Research Board
500 Fifth Street, NW
Washington, DC 20001

Biomimetic Antifreeze Molecules:
A Novel Solution to Deicing Salts and Air-Entraining Admixtures

IDEA Program Final Report

NCHRP-204

Prepared for the IDEA Program

Transportation Research Board

The National Academies

Wil V. Srubar III, Ph.D.

University of Colorado Boulder

December 31, 2019

Table of Contents

Executive Summary

The goal of this project was to synthesize and evaluate a class of low-cost, non-toxic, biodegradable antifreeze biopolymers and biomimetic small molecules. The molecules were evaluated for their effectiveness in preventing or slowing ice formation and growth on roadway and bridge surfaces during winter and as an additive to concrete in lieu of entrained air system. Stage I focused on the identification, synthesis, and characterization of biomimetic antifreeze molecules (BAMs). Polyvinyl alcohol (PVA), polyvinyl alcohol-polyethylene glycol-graft-copolymer (PVA-g-PEG), poly(2-hydroxyethyl methacrylate) (pHEMA), poly(2-hydroxypropyl methacrylamide) (pHPMA), gelatin, and folic acid, citric acid, and 2-hydroxyethyl methacrylate (HEMA) BAMs were synthesized or synthetically modified to mimic ice-binding residues and were investigated for their ice recrystallization inhibition (IRI) and freezing point depression. BAM activity was tested in deionized water as a proxy. Results suggest that BAMs in ultra-low concentrations (<0.01 mg/mL) can inhibit ice recrystallization. Smaller molecules were found to be less IRI active than larger molecules, but HEMA alone was found to depress the freezing point by 2 to 4°C at concentrations of 1 to 10 mg/mL—behavior that is similar to moderate concentrations of common deicing salts. Stage II focused on the biodegradability and cytotoxicity of BAMs. Biocompatibility of BAMs were assessed and compared to traditional deicing solutions using a LIVE/DEAD assay with human-derived dermal and lung cells. Results indicate that PVA, PVA-g-PEG, folic acid, and pHPMA perform as well as (or better than) traditional deicing solutions (i.e., NaCl, $MgCl_2$, $CaCl_2$) in the LIVE/DEAD assay. Degradability of BAMs in aqueous river water was assessed. PEG and PVA-g-PEG displayed mild degradation after 16 weeks, while PVA exhibited no degradation. Stage III focused on testing the ability of BAMs to perform as deicers and additives for freeze-thaw resistance. Additionally, PVA and PVA-g-PEG were studied for freeze-thaw resistance in ordinary portland cement (OPC) paste. While these molecules were found to be non-effective deicers, both polymers displayed freeze-thaw resistance in ordinary portland cement (OPC) paste in modified ASTM C666 testing. PVA-g-PEG modified concrete displayed freeze-thaw resistance in ASTM C666 testing.

In summary, it was found that BAMs would not effectively melt ice once it has formed nor provide additional synergistic benefit to using the molecules in tandem with traditional deicers. Contrastingly, BAMs did prevent freeze-thaw damage in cement paste and concrete. The results of this IDEA concept provide the foundational work for BAMs as an alternative to traditional air entraining agents for freeze-thaw resistance in concrete. The results of freeze-thaw testing clearly show that BAM-modified cement paste and concrete are freeze-thaw resistant and that the freeze-thaw resistance occurs with minimal air entrainment in concrete.

IDEA Product

The goal of this project was to synthesize and evaluate a class of low-cost, non-toxic, biodegradable antifreeze materials (BAMs) with behavior similar to natural antifreeze proteins found in fish, plants, insects, and bacteria for their effectiveness in preventing or slowing ice formation and growth on roadway and bridge surfaces and in cement binder during winter. As an alternative deicing solution or air entraining admixture, this product would allow for the replacement or reduced use of traditional salts that have clearly been shown to cause chloride-induced corrosion of steel and premature material failure in reinforced concrete civil infrastructure. As an additive to concrete, this product would allow for freeze-thaw resistant concrete without the need of entrained air void system.

Concept and Innovation

For 100 years, the practice of using salt (*i.e.*, NaCl, $MgCl_2$) to depress the freezing point of water to improve the safety of vehicular traffic on roadways has remained virtually unchanged. A major drawback of deicing salt application is chloride-induced corrosion of steel and premature material failure in reinforced concrete (*1-6*). Of notable importance, deicing salts offer an initially cheap solution for transportation-related applications ($900/lane-mile) to reduce collisions on icy roads; however, the annual economic costs associated with chloride-induced corrosion is in excess of $3400/lane-mile – a total annual cost for the US of $29.7B (*7-9*). Estimated annual environmental costs of deicing salts are an additional $2,300/lane-mile (*10*), bringing the total annual cost of deicing salts to more than $54B annually. In summary, although the immediate price of salt is low, the long-term economic and environmental cost is incredibly high. Thus, a novel, economically feasible salt alternative is needed to provide similar performance at lower lifecycle economic and environmental cost.

The predominant method to enhance the freeze-thaw resistance of ordinary portland cement (OPC) concrete, since the 1930s, has been to introduce an air void system. The air void system helps to reduce the pressures that develop during cyclic freezing and thawing. The stabilized air void system is created *via* the use of air entraining agents (AEAs) which behave as surfactants. In addition to enhanced freeze-thaw resistance, AEAs lead to improved workability (*11*).

Although AEAs can enhance freeze-thaw resistance they do have drawbacks including a reduction in mechanical strength, which can be as high as 6% per 1% entrained air, an increase in permeability, and set time retardation (*12-14*). Additionally, recent work has shown that once a critical saturation level, 86% to 88%, is met proper air entrainment will not prevent damage (*15*). Given the inevitable side effects and limitations related to saturation level, alternative approaches to enhance freeze-thaw resistance in cementitious materials are of particular interest.

Antifreeze proteins protect cold weather species through two primary mechanisms; ice recrystallization inhibition (IRI) and thermal hysteresis (TH) (*16*). IRI is a measure of how well a material inhibits the growth of large ice crystals (i.e. Ostwald ripening). TH is a reduction of the freezing point of ice below the equilibrium point (*16*). The specific mechanisms of IRI and TH activity are still debated but it is widely accepted that they result from the proteins interacting directly with nucleating ice (*17*). The prevention or retardation of ice growth, specifically IRI activity, was hypothesized to provide a solution that serves as a deicer for roadway surfaces and a material that reduces the damage in concrete during cyclic freeze-thaw temperatures as an additive. Proteins are not a scalable option for use at the large scales and they do not maintain their activity in non-native environments (*18*). A number of polymer and small molecules have been identified that mimic the chemical structure of antifreeze proteins and display IRI activity (*17*)

Investigation

Figure 1 provides the overall approach and steps in this investigation. Stage I focused on the identification, synthesis, and characterization of BAMs. Polyvinyl alcohol (PVA), polyvinyl alcohol-polyethylene glycol-graft-copolymer (PVA-g-PEG), poly(2-hydroxyethyl methacrylate) (pHEMA), poly(2-hydroxypropyl methacrylamide) (pHPMA), gelatin, and folic acid, citric acid, and 2-hydroxyethyl methacrylate (HEMA) BAMs were synthesized (or synthetically modified) to mimic ice-binding residues and were investigated for their ice recrystallization inhibition (IRI) and freezing point depression. BAM activity was tested in deionized water as a proxy. Stage II focused on the biodegradability and cytotoxicity of BAMs. Biocompatibility of BAMs were assessed and compared to traditional deicing solutions using a LIVE/DEAD assay with human-derived dermal and lung cells. Stage III focused on testing the ability of BAMs to perform as deicers and additives for freeze-thaw resistance. Additionally, PVA and PVA-g-PEG were studied for freeze-thaw resistance in ordinary portland cement (OPC) paste.

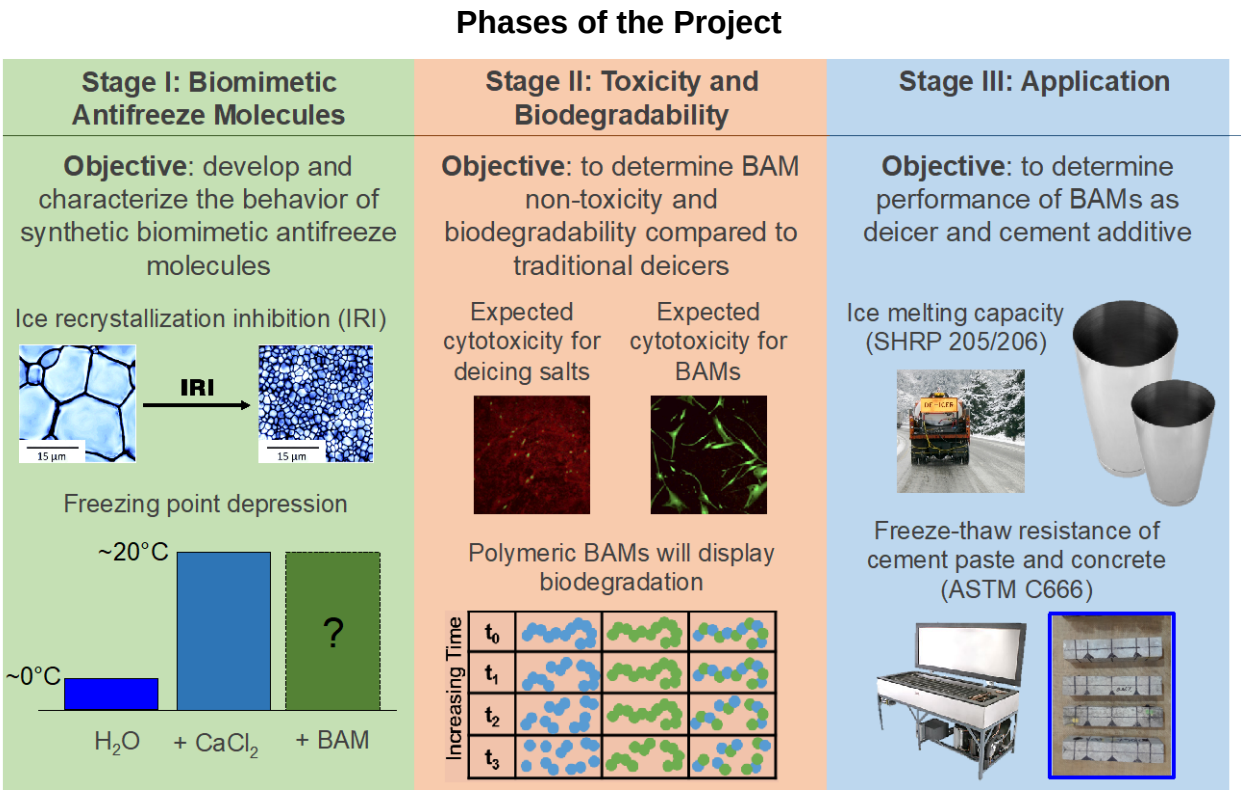

FIGURE 1: Overview of stages and objectives of the project.

Materials

Off-the-Shelf Materials

PVA, PVA-g-PEG, PEG, gelatin, folic acid, citric acid, and trehalose were identified as materials that might display IRI activity based on chemical functionalities that are similar to those of antifreeze proteins identified as responsible for IRI activity (e.g. threonine residue). All of these materials were purchased from Sigma Aldrich and used without modification.

Synthesized Materials

2-hydroxypropyl methacrylamide (HPMA) Synthesis

2-hydroxypropyl methacrylamide (HPMA) was synthesized following a previously published protocol (*19*) and the reaction scheme can be seen in **Figure 2**. In brief, dichloromethane was placed in a round bottom flask and dried with sodium carbonate as well as a nitrogen purge. The flask was cooled to -10 °C using an acetone-ice bath. D-L-1-amino-2-propanol was added to the flask followed by a nitrogen purge.

Methacryloyl chloride was loaded into dichloromethane and added dropwise to the amino-2-propanol mixture until a 1:1 molar ratio has been achieved. After the methacryloyl chloride was added, the reaction was allowed to proceed for 45 minutes at -10 °C. The reaction was then removed from the acetone-ice bath and allowed to stir as it warmed to room temperature (~1 hour). The solution was then filtered to remove the sodium bicarbonate, crystallized in DCM at -20 °C overnight and the off-white crystals collected, then recrystallized in acetone at -20 °C overnight, filtered again to collect the pure white crystals. The final product was dried and verified using ^{1}H nuclear magnetic resonance (NMR), **Figure 3**.

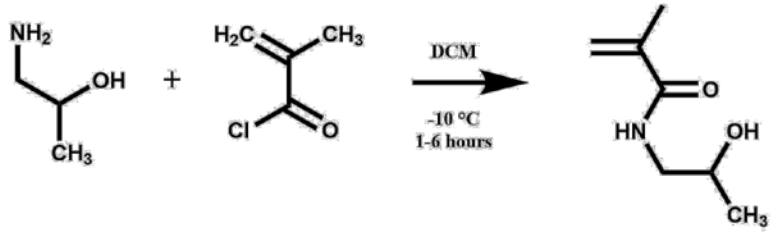

FIGURE 2: Reaction scheme of 2-hydroxypropyl methacrylamide (HPMA).

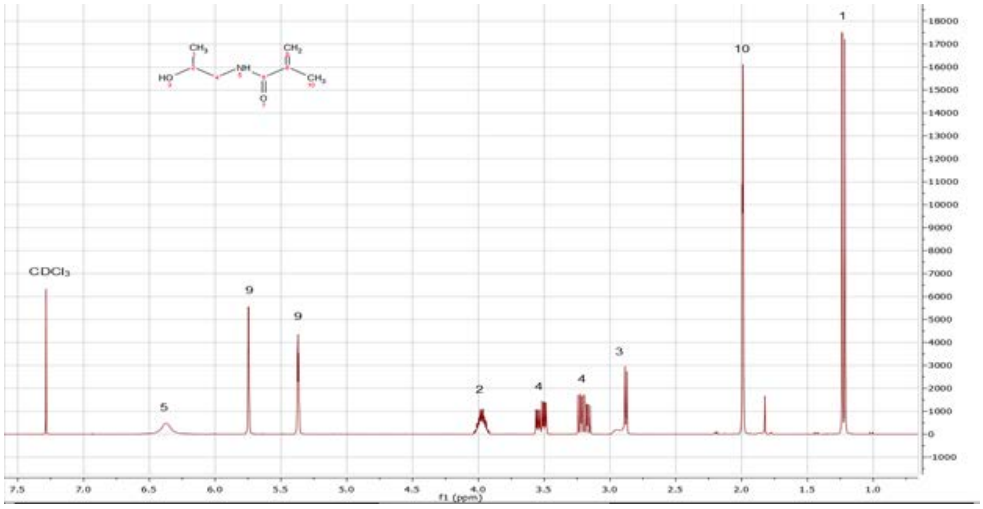

FIGURE 3: NMR results of 2-hydroxypropyl methacrylamide (HPMA) reaction.

Poly(2-hydroxy propyl methacrylamide) (pHPMA) Synthesis

Poly(2-hydroxy propyl methacrylamide) (pHPMA) was synthesized and chemically verified. It was hypothesized that it would have both IRI and TH/freezing point depression activity due to structural similarities to the amino acid threonine, the residue responsible for ice interactions on several naturally occurring ice-binding proteins (IBPs). The overall structure of the polymer is shown in **Figure 4** with the threonine reminiscent group highlighted blue. **Figure 5** provides the synthetic strategy employed to produce the polymer at both 5 and 50 kDa (Note: kDa is a measure of molecular weight).

pHPMA synthesis was confirmed with ^{1}H NMR. ^{1}H NMR data is shown in **Figure 6** while mass spectrometry data is not included in this report. The molecular weight of 5 kDa was confirmed using SEC-MALS.

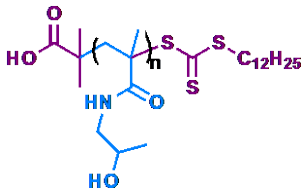

FIGURE 4: Structure of poly(2-hydroxypropyl methacrylamide), a biomimetic antifreeze polymer synthesized in-house. Side group highlighted blue is similar in structure to the amino acid threonine.

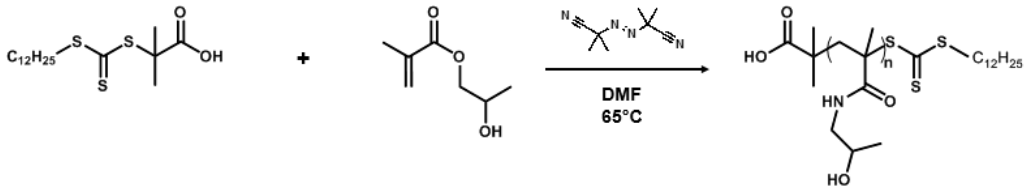

FIGURE 5: Synthetic strategy for poly(2-hydroxypropyl methacrylamide).

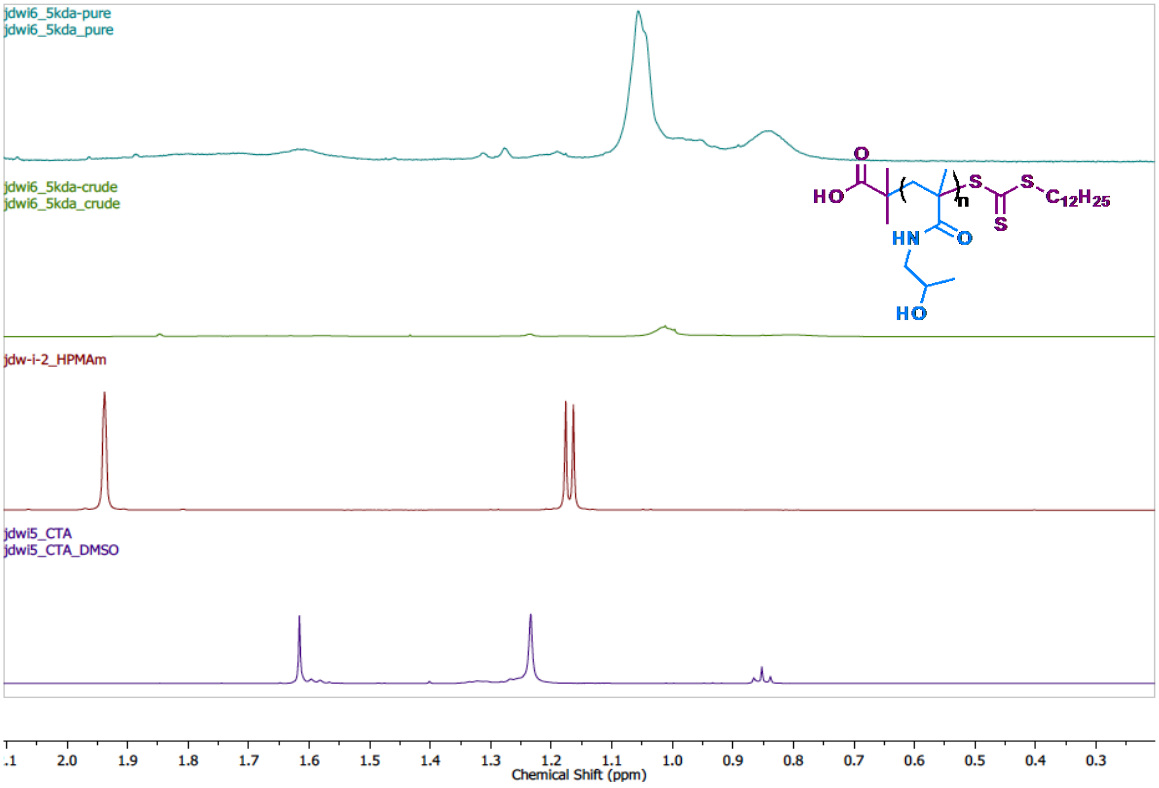

FIGURE 6: ^{1}H NMR spectra of pHPMA and associated monomers confirming synthesis.

Gelatin methacryloyl (gelMA) Synthesis

The investigators anticipated that gelatin methacryloyl (gelMA) and gelMA modified compounds could have IRI activity. GelMA synthesis is shown in **Figure 7**. Following purification, the synthesis was verified by ^{1}H nuclear magnetic resonance (NMR) shown in **Figure 8**. The peaks at 5.2 and 5.6 ppm in the top portion **Figure 8** highlighted in yellow are indicative of a successful reaction. The carbon-carbon double bond on the added methacrylamide or methacrylate functionalities can be easily modified with chemistries that are anticipated to have IRI and possibly TH activity (future work).

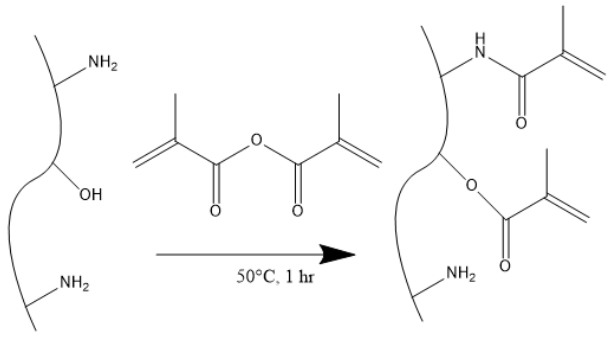

FIGURE 7: Gelatin methacryloyl (gelMA) synthesis.

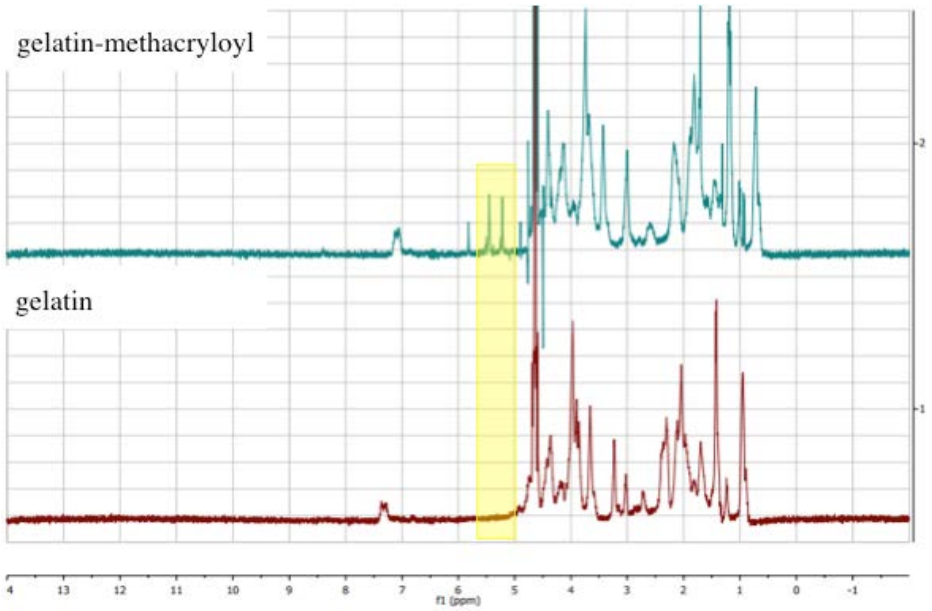

FIGURE 8: ^{1}H nuclear magnetic resonance (NMR) spectra of gelatin methacryloyl (gelMA) (blue curve) and gelatin (red curve), with the new resonances corresponding to metacryloyl highlighted in yellow.

Poly(2-hydroxyethyl methacrylate) (pHEMA) Synthesis

Figure 9a shows the synthetic strategy for the synthesis of poly(2-hydroxyethyl methacrylate) (pHEMA). **Figure 9b** shows the synthetic strategy for a polymer comprised of gelMA with a comonomer of 2-hydroxyethyl methacrylate (HEMA) to create a polymeric compound of gelMA-graft-poly(HEMA). It was anticipated that the pHEMA structure would interact with water and ice through the hydroxyl (OH) unit, and the addition of the gelMA (gelMA-g-poly(HEMA)) would demonstrate enhanced IRI activity compared to the p(HEMA) alone.

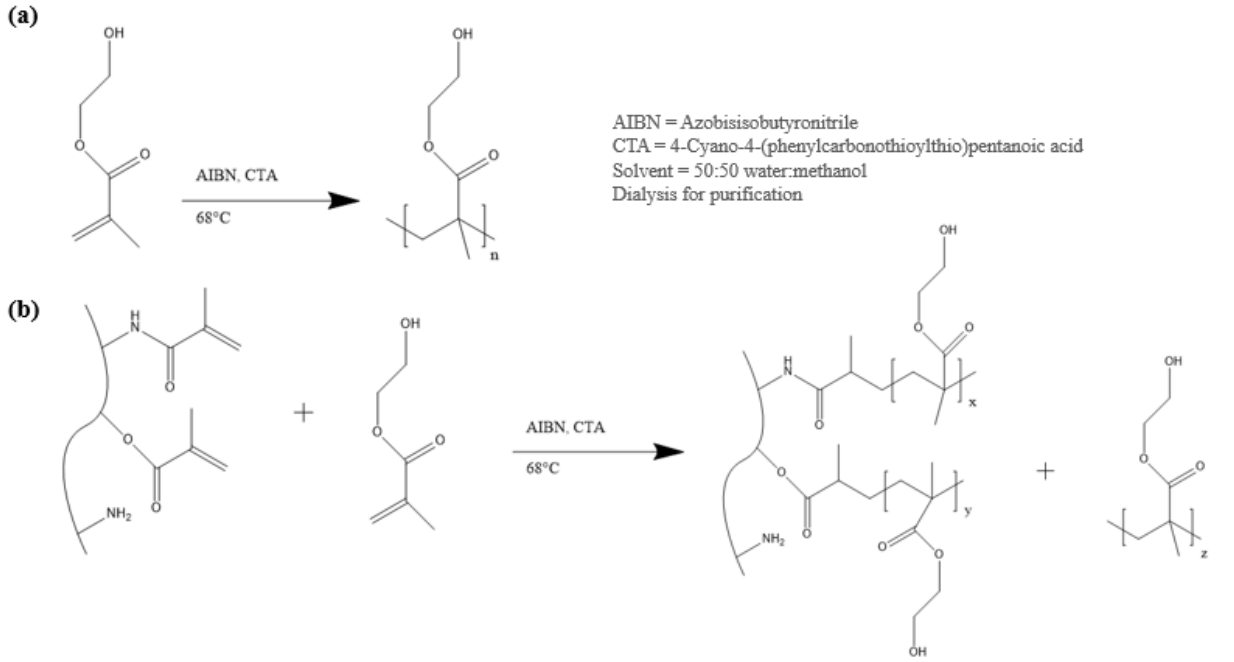

FIGURE 9: (a) Chemical structure of poly(2-hydroxyethyl methacrylate). (b) Synthetic strategy used in the synthesis of gelatin methyacryloyl-graft-poly(2-hydroxyethyl methacrylate).

Ice Recrystallization Inhibition

Ice recrystallization inhibition (IRI) activity served as the first indicator for a material's potential to serve as a deicing solution and/or as an additive to cement for freeze-thaw resistance. IRI is tested using a modified splat assay (*20*). Briefly, a 10–20 μL droplet of solution was dispensed from 1.7 m through a PVC pipe onto a microscope slide on top of an aluminum block chilled with dry ice to obtain a monolayer of ice crystals. The slide was then transferred to an Otago nanoliter osmometer sample stage and annealed at −4 °C. The temperature was monitored using a bead-type thermocouple. Images were collected immediately after the splat was transferred to the cold stage and again at 30 minutes to observe ice recrystallization. Images were obtained using an OMAX A35140U camera mounted to an Olympus BX41 microscope with ELWD U Plan 20x/0.45 objective and cross polarizers. All materials were tested with

phosphate buffer saline (PBS) as the solvent because this is the primary solvent used in literature related to IRI.

Table 1 summarizes the IRI assay results. PVA-g-PEG, pHEMA, pHPMA, folic acid, citric acid, and HPMA have not previously been reported to be IRI active. PEG has previously been reported to have no IRI activity and was used a negative control (*21*). PVA and trehalose have previously been shown to be IRI active (*22,23*). PVA is widely considered to be the most IRI active synthetic material (and most widely studied). The only material that was as IRI active, approximately 80% reduction in ice grain size compared to control, as PVA was PVA-g-PEG. A typical micrograph of a sample containing PVA-g-PEG can be found in **Figure 10**. Based on the IRI results, concentration requirements, known non-toxicity, and solubility in water PVA-g-PEG and pHPMA were chosen as polymer materials to study further. Folic acid and HPMA were chosen as small molecules to study further. Representative micrographs of other materials tested for IRI activity can be found in **Figures 11-17**. Note that no images are provided for gelatin and gelatin methacryloyl due to inability to effectively form a splat for testing.

TABLE 1: Materials tested for IRI activity

Material	**IRI Active? (Yes/No)**	**Concentration Tested in PBS**
Polyvinyl alcohol (PVA)	Yes	0.1-1 mg/mL
Polyvinyl alcohol-polyethylene glycol-graft-copolymer (PVA-g-PEG)	Yes	0.1-1 mg/mL
Polyethylene glycol (PEG)	No	0.1-1 mg/mL
Poly(2-hydroxyethyl methacrylate) (pHEMA)	Yes	2.0 mg/mL
Poly(2-hydroxypropyl methacrylamide) (pHPMA)	Yes	0.25, 0.50 mg/mL
Gelatin	No	0.1-1 mg/mL
Gelatin methacryloyl	No	0.1-1 mg/mL
Folic acid	Yes	0.01, 0.05, 0.1, 0.50 mg/mL
Citric acid	Yes	0.50 mg/mL
2-hydroxypropyl methacrylamide (HPMA)	Yes	0.1, 1.0, 10 mg/mL
Trehalose	Yes	7.5, 75 mg/mL

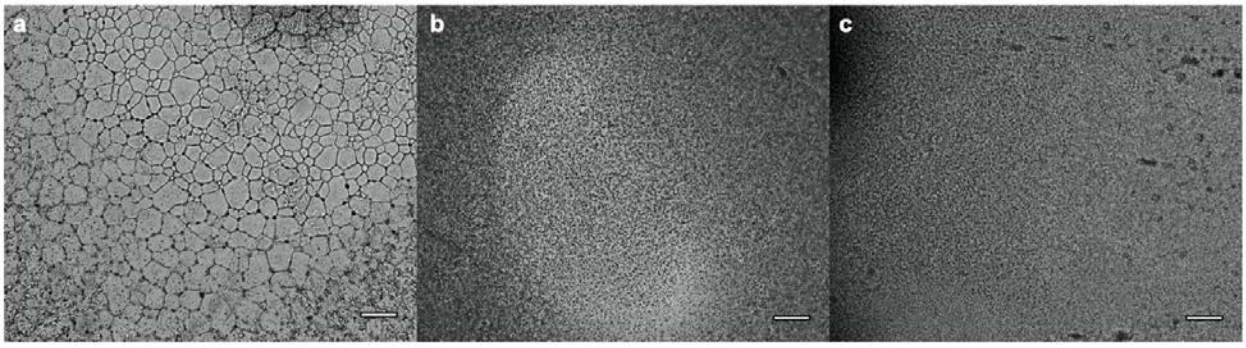

FIGURE 10: Optical micrographs of IRI splat assay for (a) PBS control solution, (b) 0.50 mg/mL PVA in PBS, and (c) 0.50 mg/mL PVA-g-PEG in PBS after 30 minutes of annealing at -4°C. Scale bars = 100 μm.

Folic acid, **Figure 11a**, was identified as a small molecule with potential for having IRI activity. In solution, folic acid, a vitamin, self-assembles into columnar, disk-like tetramers induced by hydrogen bonding between hoogsteen-type bases (on the pterin rings) and the addition of alkali metals to a solution of folic acid induces columnar phases, **Figure 11b** (*24,25*). The functional groups on the folic acid and spacing of these columnar disks enabled the hypothesis that these materials could display IRI and TH activity and their self-assembly could mimic protein structure and function. For these experiments, we tested the solutions of folic acid in dilute sodium hydroxide for IRI activity and observe a noticeable reduction in mean crystal grain size with the addition of folic acid. This preliminary work provides confidence that this compound could serve to effectively control ice crystal grain size and given that it is commercially used as a vitamin, would be inherently safe toward humans.

The IRI activity of folic acid in DI water was tested at concentrations of 0.01 mg/mL, 0.05 mg/mL, and 0.5 mg/mL. The IRI activity in water without the presence of 1 M NaOH was further tested to confirm that the compound maintains activity. The mean largest grain size (n=10) was reduced by 25%, 50%, and 55% for 0.01 mg/mL, 0.05 mg/mL, and 0.5 mg/mL folic acid respectively when compared to just DI water. This is an important finding because it shows that the self-assembled structure, **Figure 11 b**, is not required for IRI activity. This work provides confidence that this compound could serve to effectively control ice crystal grain size and given that it is commercially used as a vitamin, would be inherently safe toward humans (also supported by previously performed toxicity study).

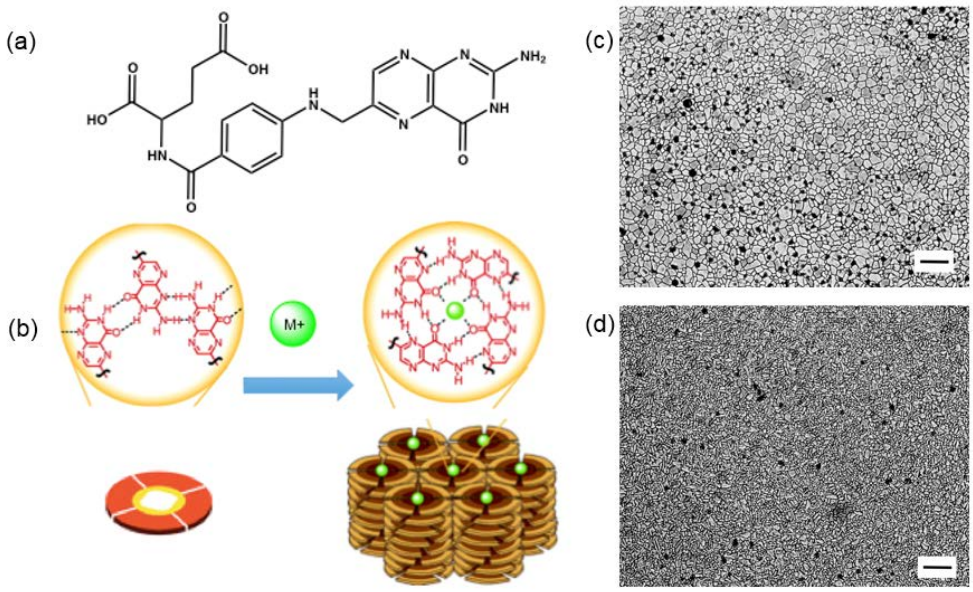

FIGURE 11: (a) Chemical structure of folic acid compound. (b) Disk shape self-assembled folic acid structure on the left and columnar self-assembled structures in the presence of alkali metals on the right. (c) Micrograph of DI water showing ice crystals with sizes of approximately 20 to 70 μm after 30 minutes of annealing at -4°C. (d) Micrograph of 0.1 mg/mL folic acid in NaOH solution showing ice crystals with a reduction in size of ~50% when compared to DI water after 30 minutes of annealing at -4°C. Scale bars are 100 μm. (b) is adopted from (*24*) and (*25*).

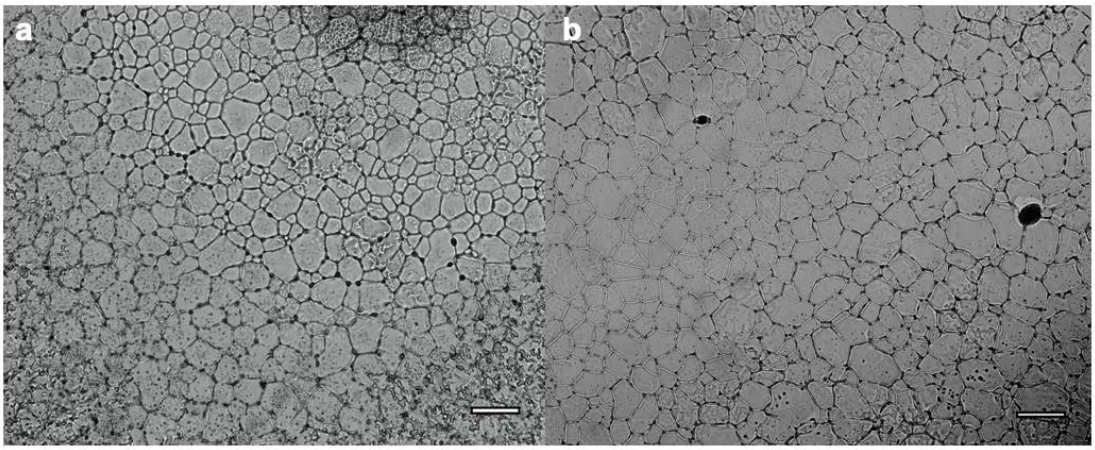

FIGURE 12: Optical micrographs of IRI splat assay for (a) PBS and (b) 0.50 mg/mL PEG in PBS after 30 minutes of annealing at -4°C. Scale bars = 100 μm.

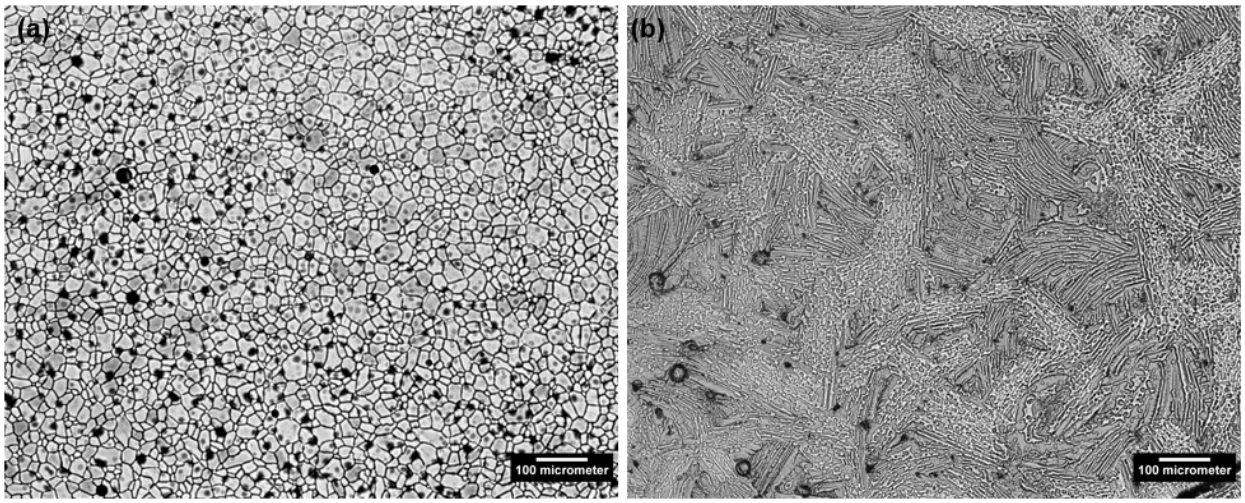

FIGURE 13: (a) micrograph of DI water showing ice crystals with sizes of approximately 20 to 70 μm after 30 minutes of annealing at -4 °C. (b) micrograph of 2 mg/mL pHEMA in DI water after 30 minutes of annealing at -4 °C showing regions with IRI activity (grains sizes <15 μm) and regions with feathering which is common in the presence of higher concentrations of IRI active materials. Scale bars are 100 μm.

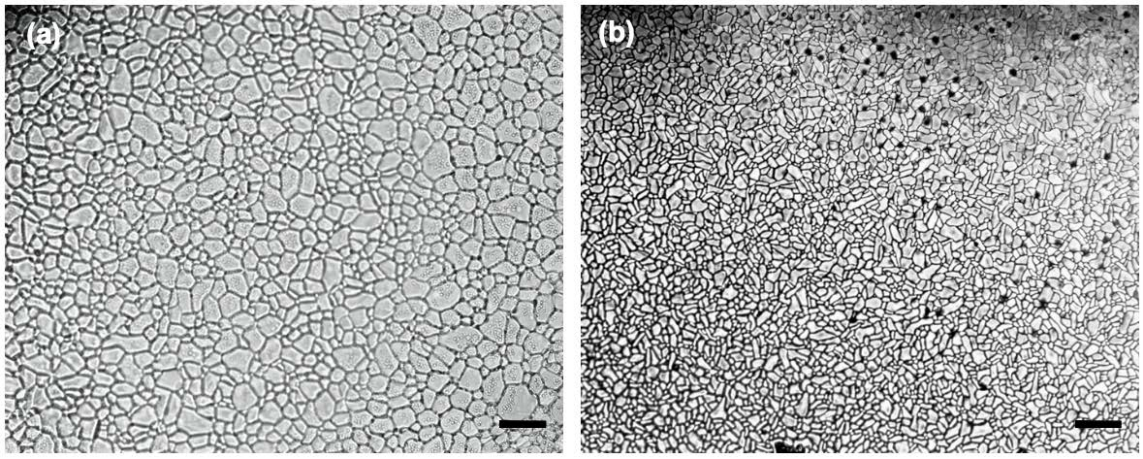

FIGURE 14: IRI experiment of 2.5 kDa in PBS solution, (a) micrograph of PBS showing ice crystals with sizes of approximately 50 to 70 μm after 30 minutes of annealing at -4 °C. (b) micrograph of 0.1 mg/mL p(HPMA) showing ice crystals with sizes of approximately 15 to 40 μm after 30 minutes of annealing at -4 °C. Scale bar is 100 μm in both micrographs.

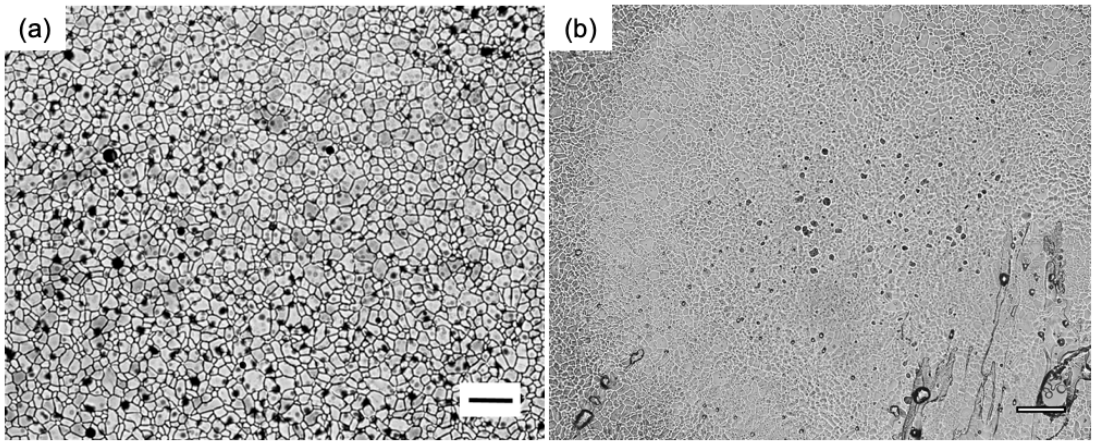

FIGURE 15: Optical micrographs of IRI splat assay for (a) DI water and (b) 0.50 mg/mL citric acid in DI water after 30 minutes of annealing at -4°C. Scale bars = 100 μm.

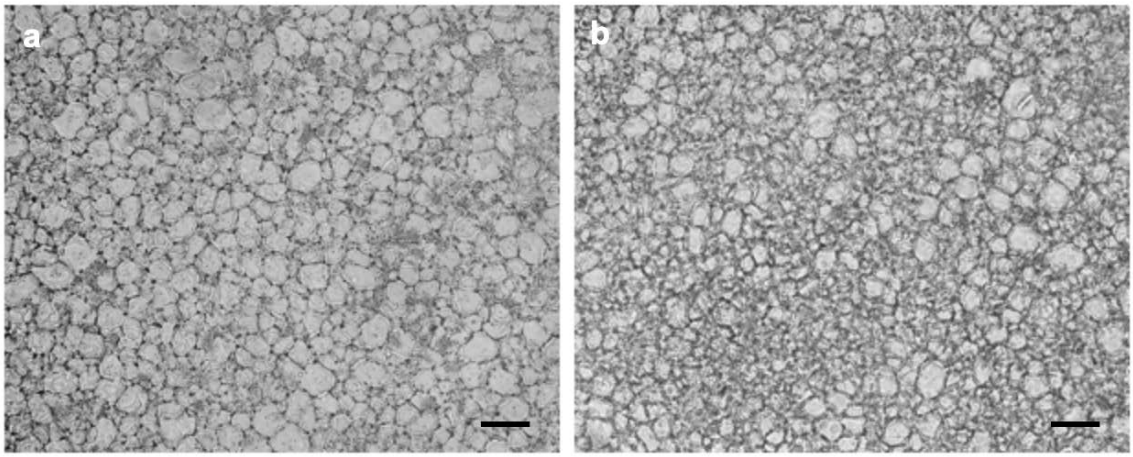

FIGURE 16: Optical micrographs of IRI splat assay for (a) PBS and (b) 10 mg/mL HPMA in PBS water after 30 minutes of annealing at -4°C. Scale bars = 100 μm.

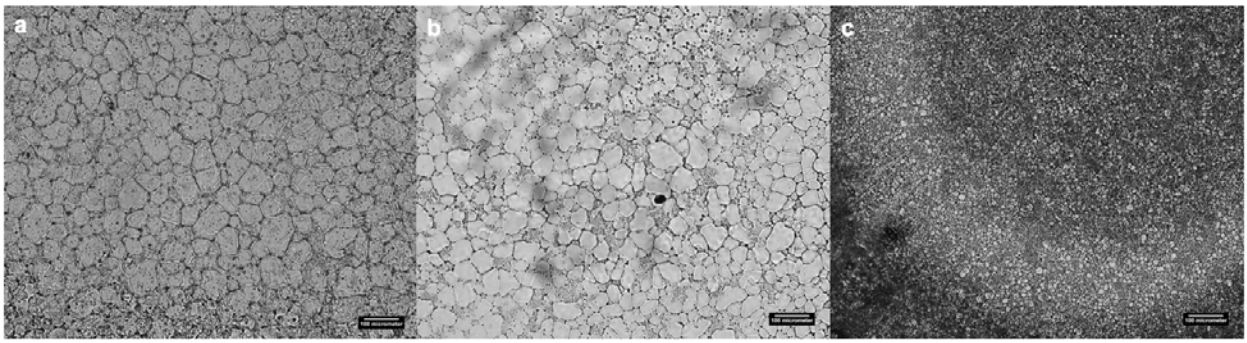

FIGURE 17: Optical micrographs of IRI splat assay for (a) PBS, (b) 7.5 mg/mL trehalose in PBS, and (c) 75 mg/mL trehalose in PBS after 30 minutes of annealing at -4°C. Scale bars = 100 μm.

Freezing Point Depression

Freezing point depression is the property responsible for traditional deicing salts effectiveness. One method to measure freezing point depression is through the use of differential scanning calorimetry (DSC) (*26*). DSC measures the energy associated with phase transitions of materials by monitoring heat flow of the sample compared to a control sample. Liquid samples were exposed to two cycles of heating and cooling, 25°C to -60°C at 2°C/min. During the heating cycle, the characteristic peak can be determined. The characteristic peak is essentially the beginning of ice crystal formation and can be considered the effective temperature for a given deicing solution (*26*). **Figure 18** provides a representative DSC thermogram showing the characteristic peak.

Table 2 summarizes the materials tested for freezing point depression. 12wt% NaCl, 13.5wt% $MgCl_2$, and 15.0wt% $CaCl_2$ were all tested for comparison. **Figures 19-23** provide a selection of DSC thermograms for other materials tested.

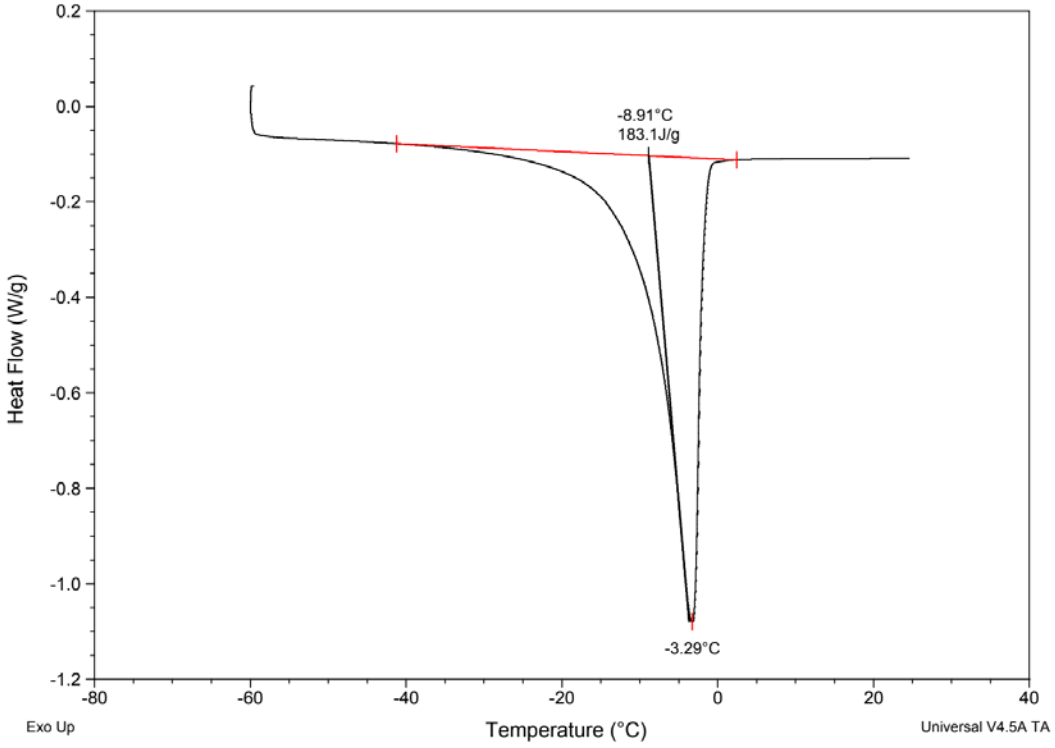

FIGURE 18: DSC thermogram of 1 mg/mL PVA in 13.5wt% $MgCl_2$ solution showing the characteristic peak that corresponds to the formation of ice crystals. Note that the peak labeled -3.29°C represents the characteristic peak.

TABLE 2: Materials tested for freezing point depression using DSC. Calculated characteristic peak for material are provided.

Material	**Average Characteristic Peak Temperature (°C)**	**Concentration**
NaCl	-7.7	12.0wt%
$MgCl_2$	-3.1	13.5wt%
$CaCl_2$	-10.9	15.0wt%
PVA-g-PEG in DI	1.6	1 mg/mL
PVA-g-PEG in 12.0wt% NaCl	-7.0	1 mg/mL
PVA-g-PEG in 13.5wt% $MgCl_2$	-3.5	1 mg/mL
PVA-g-PEG in 15.0wt% $CaCl_2$	-11.0	1 mg/mL
PVA in DI	1.3	1 mg/mL
PVA in 12.0wt% NaCl	-6.4	1 mg/mL
PVA in 13.5wt% $MgCl_2$	-3.1	1 mg/mL
PVA in 15.0wt% $CaCl_2$	-3.3**	1 mg/mL
pHPMA	0.5	10 mg/mL
HPMA*	-2.6	1 mg/mL
HPMA*	-4.6	10 mg/mL

*Note: HPMA was tested in PBS and not in DI water.

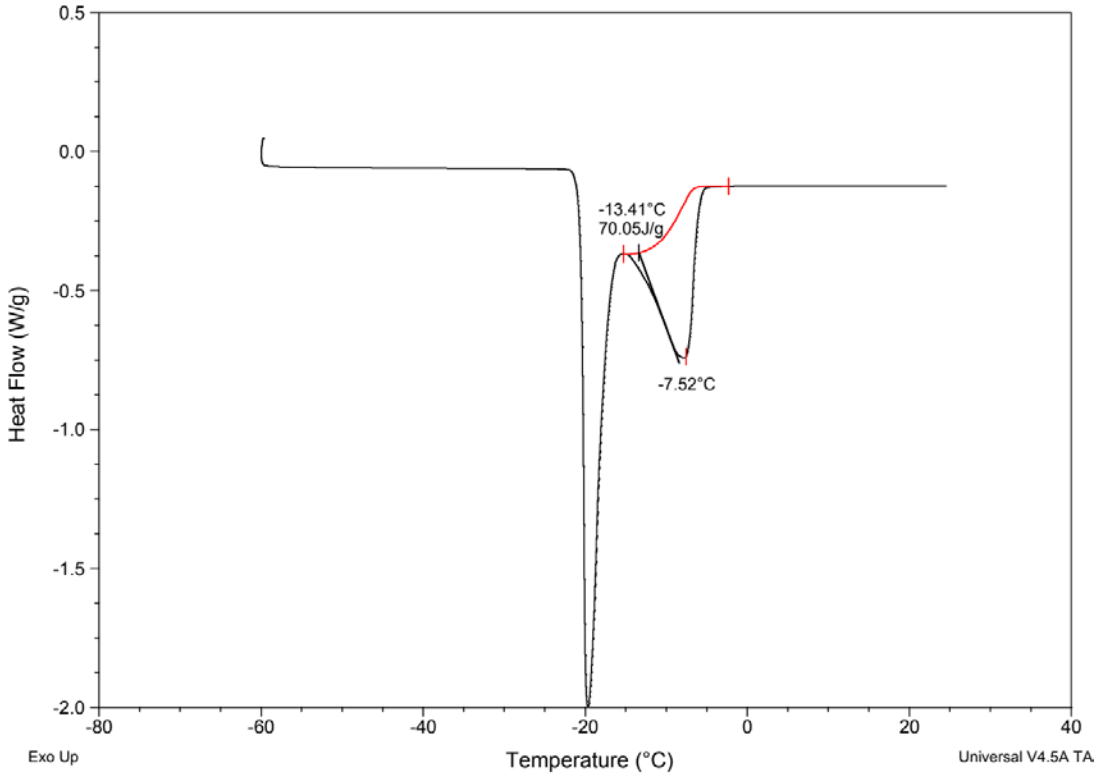

FIGURE 19: DSC thermogram of 12.0wt% NaCl solution

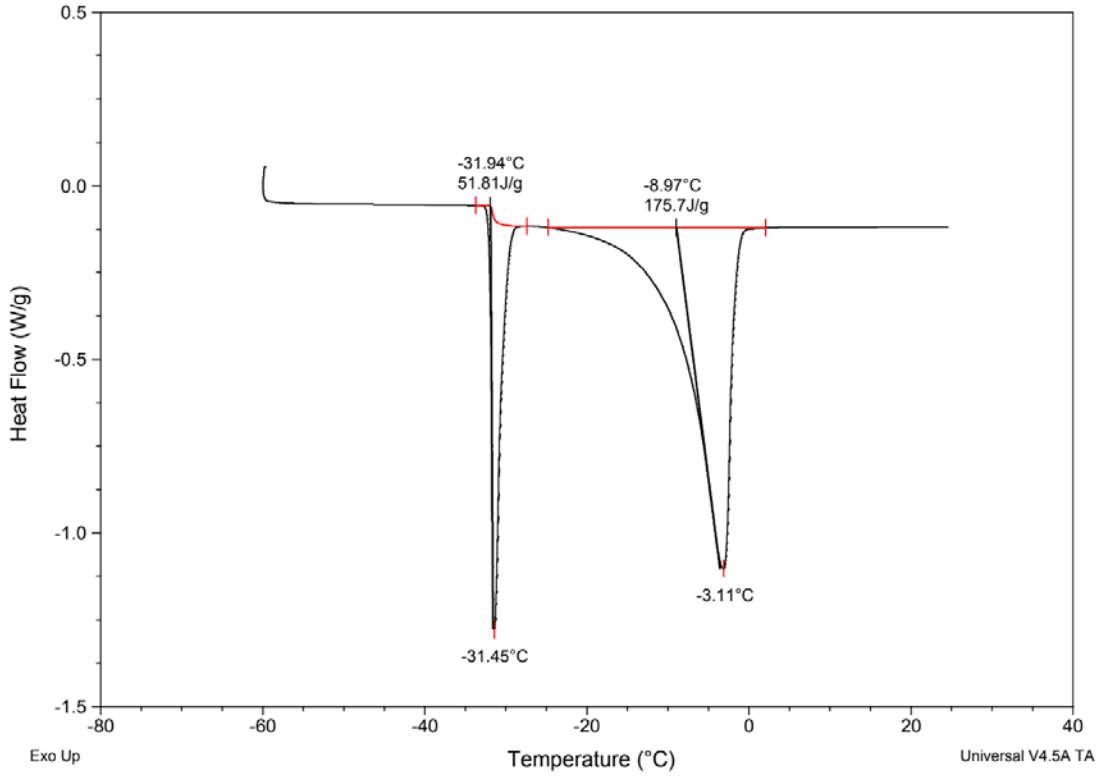

FIGURE 20: DSC thermogram of 13.5wt% $MgCl_2$ solution.

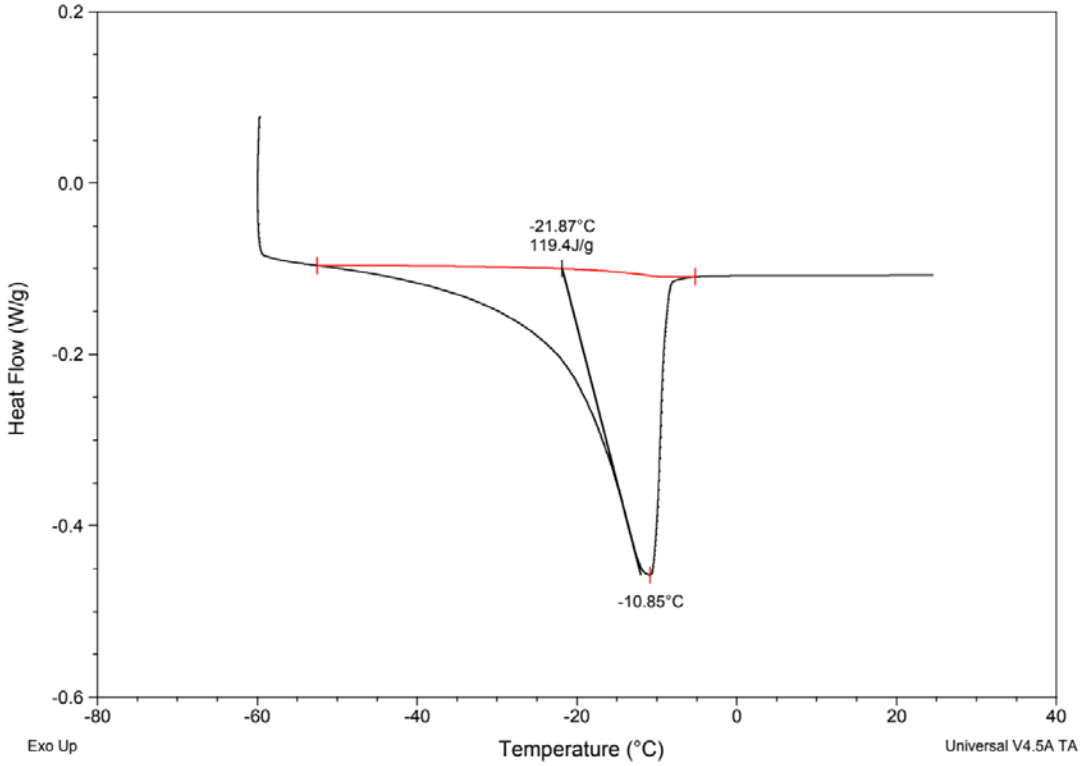

FIGURE 21: DSC thermogram of 15.0wt% $CaCl_2$ solution.

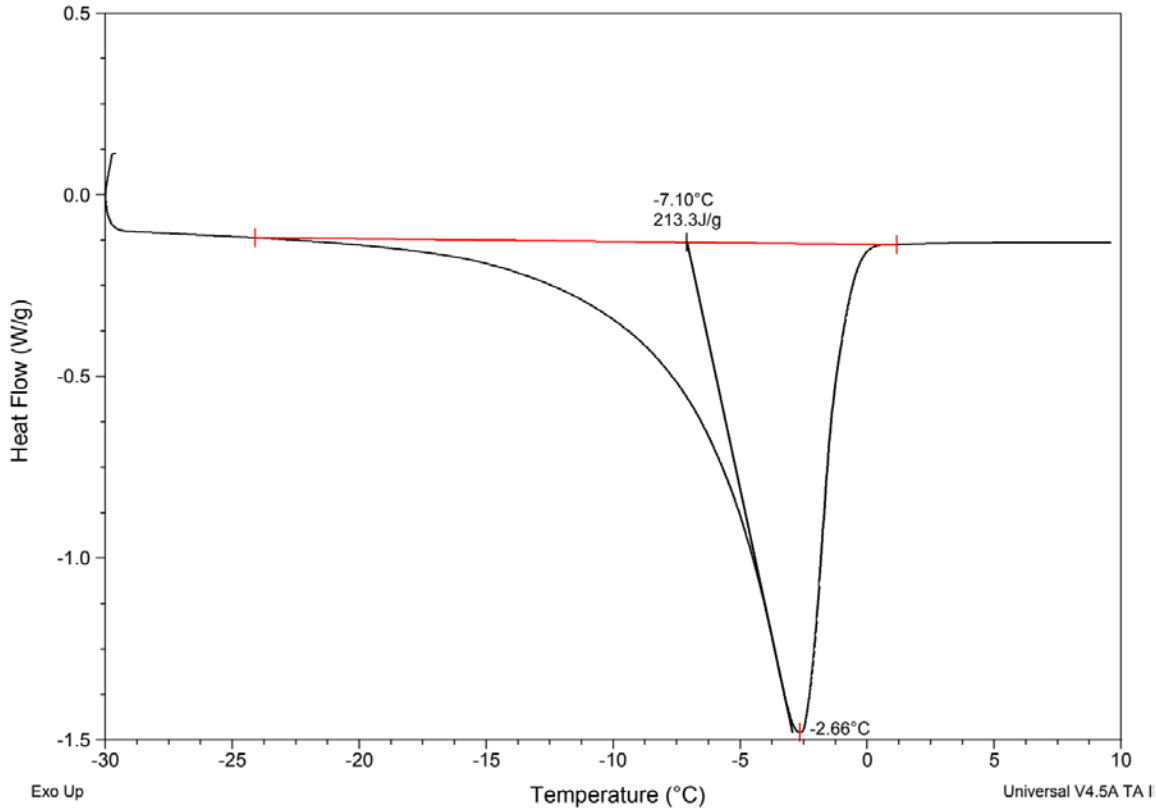

FIGURE 22: DSC thermogram of 10 mg/mL HPMA in PBS.

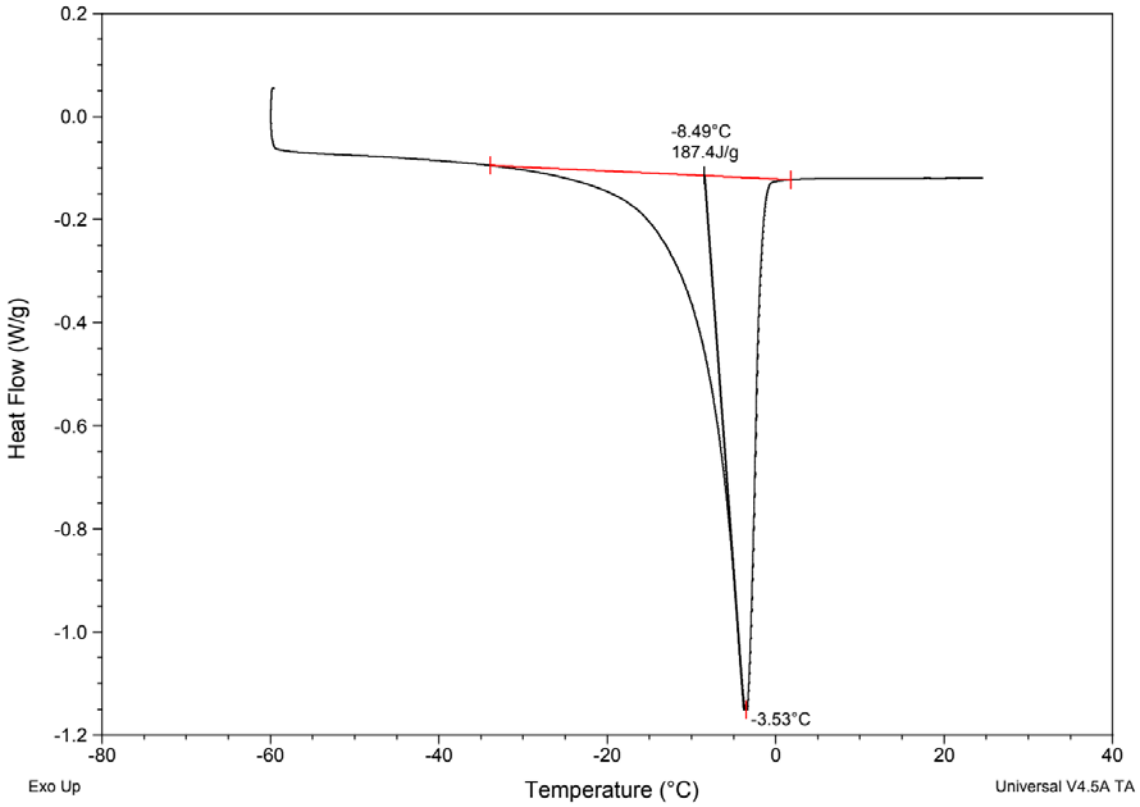

FIGURE 23: DSC thermogram of 1 mg/mL PVA-g-PEG in 13.5wt% $MgCl_2$ solution.

Toxicity

It is prudent to investigate the toxicity of the current and the proposed technology against human derived lung and skin cells to provide an indication of potential toxicity against these organs moving forward. The toxicity of deicing salts and solutions as well as our material candidates were evaluated using a semi-quantitative cellular assay (LIVE/DEAD viability assay). In the assay, both the alive and dead components of the cell are monitored with dyes that respond to metabolic components for live cells (in green) and dead cells (in red). For these experiments, human derived lung (IMR-90) and human dermal fibroblast (HDFn) cell lines were used.

The IMR-90 cells were incubated with $CaCl_2$, $MgCl_2$, NaCl, commercially available $CaCl_2$ deicing solution ($CaCl_2$ Deicing Solution), and commercially available $MgCl_2$ deicing solution (Liquid Deicing Solution), PEG, PVA, PVA-g-PEG, and pHPMA for 24 hours at a concentration of 10 mg/mL and 1 mg/mL then stained with the LIVE/DEAD stain and imaged. The results of the assay are included in **Figure 24** for the 10 mg/mL and 1 mg/mL concentrations. It is anticipated that lung cells would be exposed to these components when the material is made into an aerosol when repeatedly run over by cars or upon spreading. It is notable that the concentration tested is much lower than would be expected when

the salts are spread on a road. From the data, it appears that the $CaCl_2$ salt causes the most cell death, evidenced by low cell counts and primarily red cells. The deicing solution and material candidates show primarily live cells with some evidence of dead cells at the 10 mg/mL solution. At 1 mg/mL, all solutions appear non-toxic to human derived lung cells. These results indicate that proposed material technologies have toxicity to human derived lung cells as well or better than commercial deicing solutions and better than $CaCl_2$ salt.

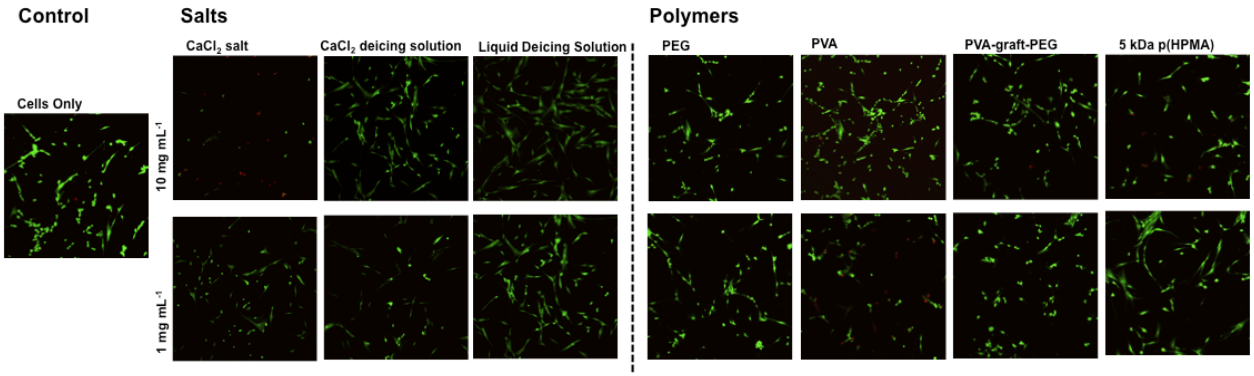

FIGURE 24: The experimental results of the LIVE DEAD viability assay using a human derived lung cell line (IMR-90). The cellular control is to the left of the figure. The top row of images is 10 mg/mL with the name for each tested component listed above, the bottom row of images are cells exposed to a concentration of 1 mg/mL.

The HDFn cells were incubated with $CaCl_2$, $MgCl_2$, NaCl, commercially available $CaCl_2$ deicing solution ($CaCl_2$ Deicing Solution), and commercially available $MgCl_2$ deicing solution (Liquid Deicing Solution), PEG, PVA, PVA-g-PEG, pHPMA, and folic acid for 24 hours. All materials were tested at a concentration of 50 mg/mL and 10 mg/mL, with the exception of folic acid which was only tested at 50 mg/mL, then stained with the LIVE/DEAD stain and imaged. Higher concentrations were used for the HDFn cell line due to the likelihood that skin exposure would occur at higher concentrations than lung exposure. The results of the assay are included in **Figure 25** for the 50 mg/mL and **Figure 26** 10 mg/mL concentration. PEG, PVA, and PVA-g-PEG show primarily live cells at both the 50 mg/mL and 10mg/mL solution. pHPMA shows primarily dead cells at 50 mg/mL but primarily live cells at 10 mg/mL. The liquid deicing solution showed some live cells at both concentrations which is likely due to it containing agriculture by products (in addition to $MgCl_2$). The $CaCl_2$ deicing solution shows primarily dead cells at both 50 mg/mL and 10 mg/mL. Of the three salts tested, $MgCl_2$ was the least toxic but all three were toxic at 50 mg/mL. These results indicate that proposed material technologies have toxicity to human dermal cells as well or better than commercial deicing solutions and better than $CaCl_2$, $MgCl_2$, and NaCl salts.

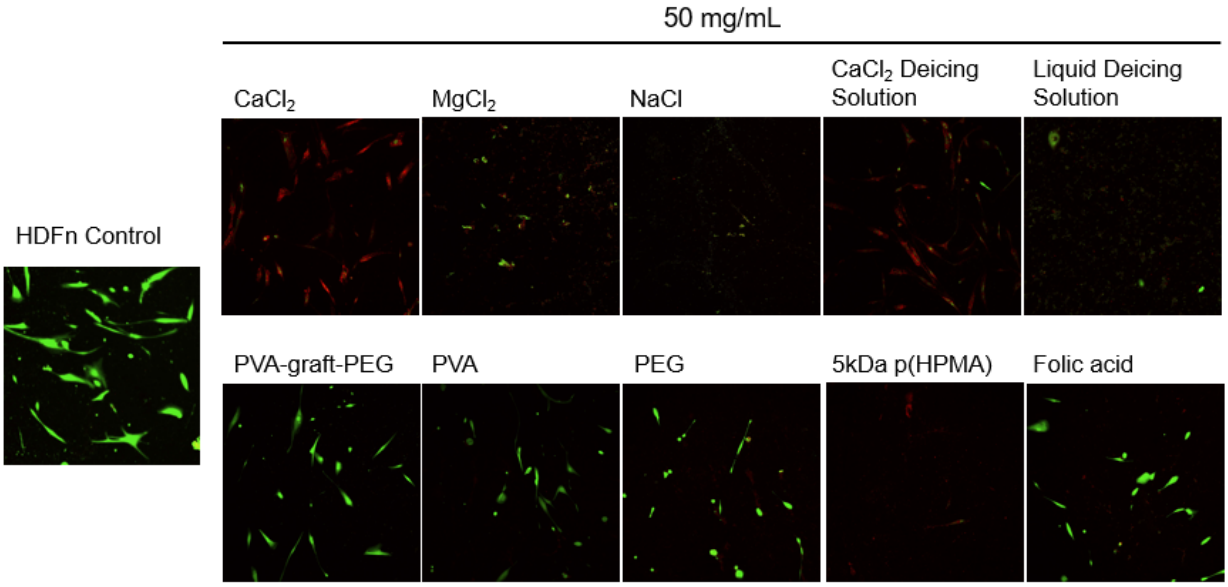

FIGURE 25: The experimental results of the LIVE DEAD viability assay using a human dermal fibroblast cell line (HDFn) and materials added at 50 mg/mL. The cellular control is to the left of the figure. The name for each tested component listed above.

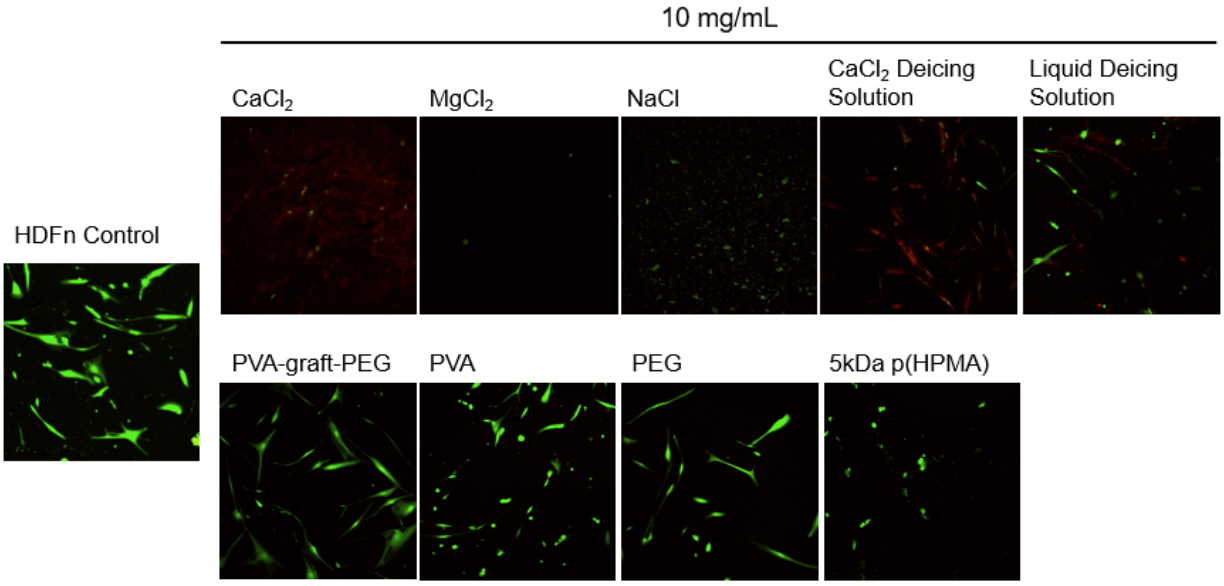

FIGURE 26. The experimental results of the LIVE DEAD viability assay using a human dermal fibroblast cell line (HDFn) and materials added at 10 mg/mL. The cellular control is to the left of the figure. The name for each tested component listed above.

Biodegradability

The biodegradability of polymeric candidates was evaluated by monitoring their molecular weight change while incubated in locally collected river water at ambient lab conditions over the course of 16 weeks. A

decrease in molecular weight would indicate that the polymers have degraded. Aliquots were collected every week and molecular weight monitored by a size exclusion chromatography multi-angle light scattering (SEC-MALS) instrument. The biodegradability of two polymeric candidates (PVA and PVA-g-PEG) and one polymeric control (PEG) was completed. pHPMA was not included in the testing due to material availability. However, HPMA and pHPMA are both known to be non-immunogenic and non-toxic.

Polymers were loaded at a concentration of 20 mg/ml into local river water (RW) and allowed to stir at ambient temperature. Aliquots were collected after 1 day, 2 days, 1 week, 2 weeks, 3 weeks, 6 weeks, 8 weeks, and 16 weeks of exposure to RW. These aliquots are stored in -20°C until the 16 week time point was reached at which point all aliquots were analyzed on a size exclusion chromatography multi-angle light scattering (SEC-MALS) instrument to observe any changes in molecular weight.

The initial molecular weight and polydispersity of the polymers were determined by analyzing a freshly made sample using size-exclusion chromatography (SEC) system equipped with a multi-angle light scattering (MALS) detector, an ultraviolet (UV) detector monitoring at 220 nm, and a refractive index (RI) detector. The mobile phase was deionized water at a flow rate of 0.4 mL/min. 50 µL of each sample were analyzed (20 µg polymer/injection).

Spectra for PEG, PVA, and PVA-g-PEG can be found in **Figures 27**-**29** respectively. As light scattering peaks are present between 10-20 minutes on all spectra, it can be assumed that remnants of particles from the river water used were observed. This assumption was corroborated by the calculated hydrodynamic radius of those particles (25-50 nm), which are too large for the anticipated polymer sizes used in this study.

For refractive index (RI), each polymer demonstrated a single, dominant peak (**Figure 27**-**29**). For the PVA RI, although intensity changed, it is not expected that the polymer degraded. Since elution time indicated polymer size, the change in intensity is likely due to random sampling of the degradation aliquot. Similar arguments can be made for the PEG, and PVA-g-PEG samples.

For light-scattering (LS), PEG demonstrates a peak between 30-35 minutes (**Figure 27**), which is notably absent in the 16 week LS trace. Similarly, the PVA-g-PEG shows a peak in the same location at 1 day, and that peak is absent after 16 weeks. PVA does not seem to have any differences in LS signal.

It is assumed that the PEG and PVA-g-PEG polymers are exhibiting some level of degradation, albeit slowly. This degradation is attributed to the oxide linkage in PEG that is more susceptible to aqueous degradation.

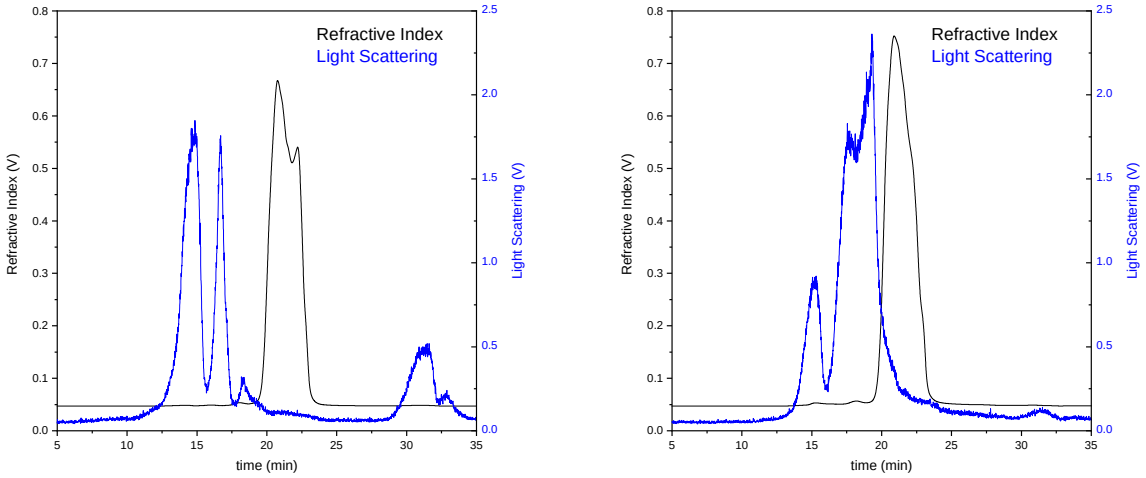

FIGURE 27. PEG Refractive Index and Light Scattering for Day 1 (*left*) and Week 16 (*right*).

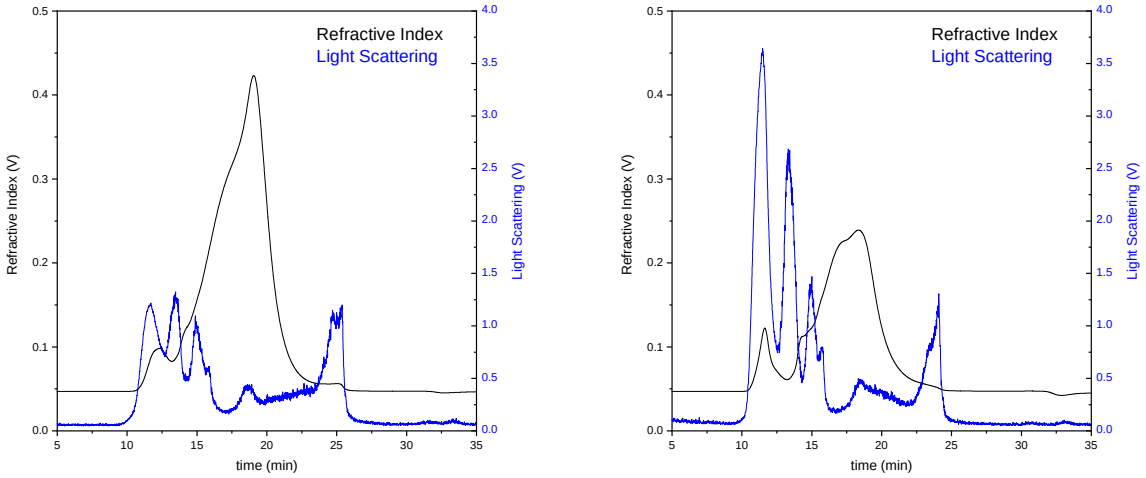

FIGURE 28. PVA Refractive Index and Light Scattering for Day 1 (*left*) and Week 16 (*right*).

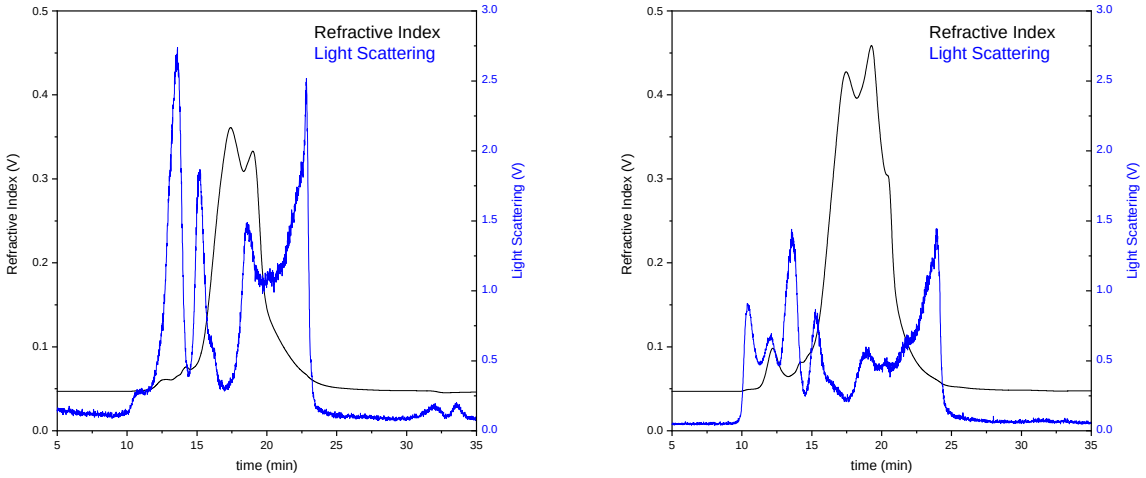

FIGURE 29. PVA-g-PEG Refractive Index and Light Scattering for Day 1 (*left*) and Week 16 (*right*).

Ice Melting Capacity

Ice melting capacity is a technique used to assess the ability of deicing solutions. The Strategic Highway Research Program (SHRP) published methods to measure the ice melting capacity, SHRP H205.1 and H205.2 (*26*) and (*27*). Additionally, Gerbino-Bevins et al. (*28*) reported a modified version of the SHRP method, shaker method, that utilizes a device to measure the ice melting capacity of deicing solutions. This method was first adopted for the project. The method is briefly described here. 7 mL of deicing solution are placed in an insulated container with a cap that allows liquid to drain into the main compartment while filtering solids. Ice cubes of known mass are weighed and placed into a freezer. The container with deicing solution is also placed in the freezer. After acclimation for a minimum of 6 hours, the ice is added to the container and shaken for 5 minutes. The device is then placed in the freezer for 5 minutes so that the liquid drains into the cap. Finally, the ice is removed and weighted into a pre-weighed beaker. The amount of melted ice is calculated, and the capacity is reported as grams of ice melted per mL of deicer.

The ice melting capacity was previously studied using the shaker method. The team found that the variability in the results was too large. Due to this, the method described in SHRP H205.1 and H205.2 were used for determination of ice melting capacity was adopted. NaCl, $CaCl_2$, and $MgCl_2$ solutions were prepared and used to compare the proposed materials. Based on the freezing point depression results it was anticipated that negligible enhancement would result from the addition of the BAMs except HPMA. **Table 3** provides a summary of the ice melting capacity for deicers tested at -1°C 60 minutes after

application. PVA-g-PEG solutions were found to provide no ice melting capacity and when combined with a common deicer salt (NaCl, $CaCl_2$, or $MgCl_2$) no enhancement was observed.

TABLE 3: Ice melting capacity of deicers at -1°C 60 mins. after application. Note that n=3 for each deicer.

Material	**Average Ice Melting Capacity (g ice/g deicer)**
12.0 wt.% NaCl	4.73
13.5 wt.% $MgCl_2$	7.00
15.0 wt.% $CaCl_2$	3.28
$MgCl_2$ based deicer solution (1.5:1 dilution)	4.61
$CaCl_2$ based deicer solution (1.5:1 dilution)	4.89
PVA-g-PEG (1 mg/mL)	0.00
PVA-g-PEG 1 mg/mL in $MgCl_2$ based deicer solution (1.5:1 dilution)	2.23
PVA-g-PEG 1 mg/mL in $CaCl_2$ based deicer solution (1.5:1 dilution)	3.29
HPMA (1 mg/mL)	0.00
HPMA (10 mg/mL)	0.00

Freeze-Thaw Resistance

Poly(vinyl alcohol)-poly(ethylene glycol) graft copolymer (PVA-g-PEG) in Paste

The team investigated the ability of PVA-g-PEG to enhance the freeze-thaw resistance of Type I/II ordinary portland cement (OPC) paste. PVA-g-PEG was chosen due to its high solubility in water. Cement paste samples (32 mm in height and 16 mm in diameter) at a water to cement ratio of 0.42 were prepared with an addition of PVA-g-PEG and PEG at 0.010 and 0.021 wt.% of cement. These additions correspond to 0.25 mg/mL and 0.5 mg/mL PVA-g-PEG and PEG in water which were previously tested for IRI activity. PEG has no IRI activity and acts as a negative control. After 14 days of curing at 100%

relative humidity, the samples (including a 0.42 w/c control sample with no polymer addition) were subjected to cyclic freezing and thawing conditions.

All samples containing an addition of PVA-g-PEG at 0.021 wt.% of cement showed no damage after freeze-thaw cycling. Damage was assessed visually (scaling and spalling) and by identification of internal cracks with micro X-ray computed tomography (MXCT). **Figure 30** shows both bulk sample and a representative MXCT 2D cross-section image of the control, PEG at 0.021 wt.% of cement, and PVA-g-PEG at 0.021 wt.% of cement. Spalling and internal cracks are clearly present in all samples except those containing PVA-g-PEG.

The air content of the hardened paste samples was determined from the MXCT scans. Dragonfly 3.5 software was used to create 3D reconstructions, identify air voids, and calculate the volume of air voids in the scanned portion of the paste samples (air content). **Figure 31** shows the 3D reconstructions with the air voids system highlighted in pink. Below each reconstruction is the hardened state air content. The samples all had an air content below 1% which is well below the 16-25% recommended air content for cement paste (*29*). This is a critical finding because it suggests that PVA-g-PEG provides freeze-thaw resistance without an air void system.

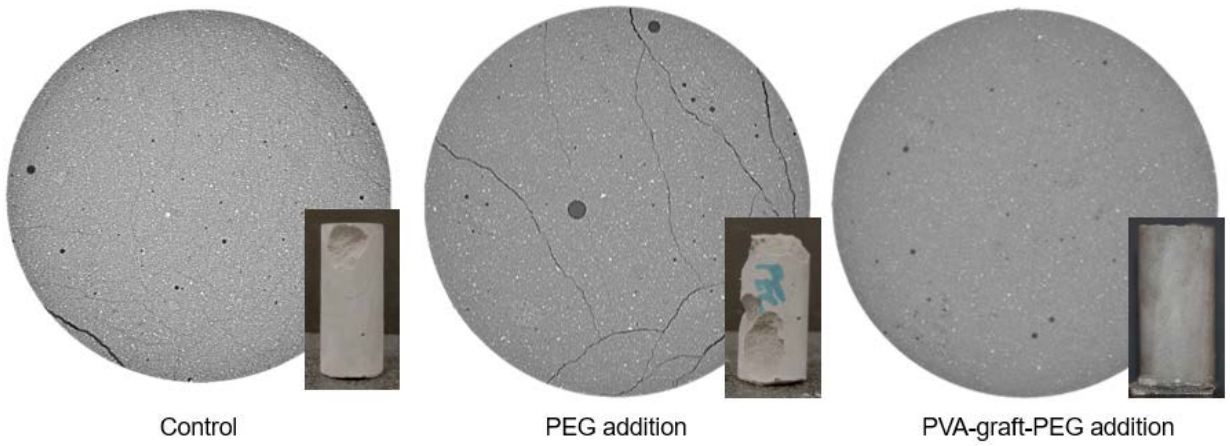

FIGURE 30: Post freeze-thaw MXCT 2D cross-sectional images of control, PEG at 0.021 wt.% of cement addition, and PVA-g-PEG at 0.021 wt.% of cement addition. Inset images show bulk samples post freeze-thaw. MXCT cross-sections are 9 mm in diameter. Bulk samples are 16 mm in diameter by 32 mm in height.

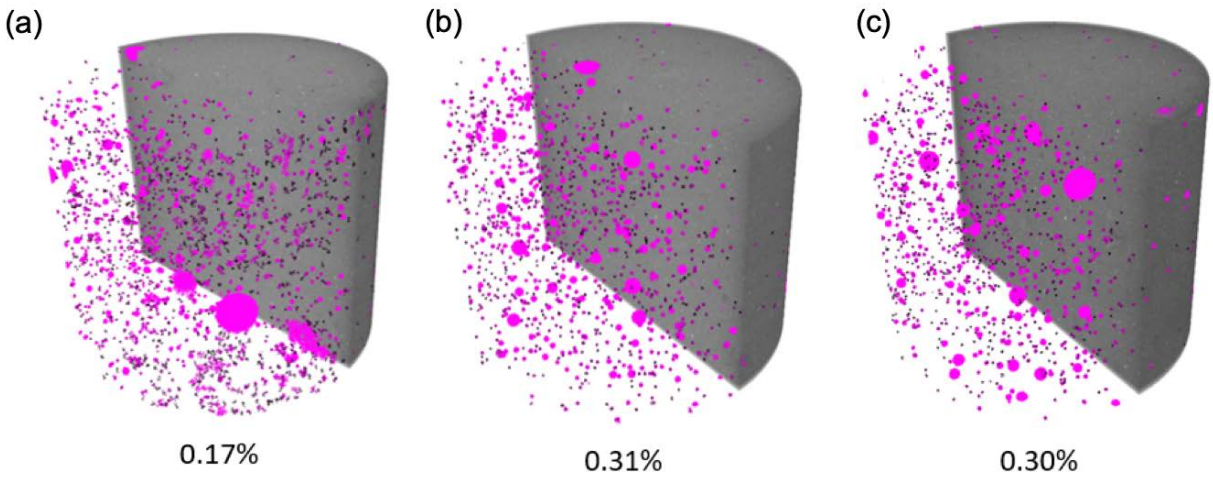

FIGURE 31: MXCT 3D reconstructions showing the air void system highlighted in pink. (a) control, (b) PEG at 0.021 wt.% of cement addition, (c) PVA-g-PVA at 0.021 wt.% of cement addition. Below each sample is the calculated hardened state air content of paste samples.

Poly(vinyl alcohol)-poly(ethylene glycol) graft copolymer (PVA-g-PEG) in Concrete

The ability of PVA-g-PEG to enhance the freeze-thaw resistance of OPC concrete was investigated. Cylindrical and prismatic concrete samples were prepared following the mix design shown in **Table 4**. PVA-g-PEG was found to perform best at a dosage of 0.066 wt.% of cement. The PVA-g-PEG modified concrete was tested along with samples containing a commercially available air entraining agent. Samples were prepared and cured according to ASTM C192, ASTM C511, and ASTM C666 (*30*-*32*). Freeze-thaw cycling was performed following ASTM C666 Procedure A (*32*).

Freeze-thaw resistance were assessed by measuring the relative dynamic modulus of elasticity, durability factor, and length change. Additionally, the fresh state air content, hardened state air content, and spacing factor were determined. All samples containing an addition of PVA-g-PEG at 0.021 wt.% of cement showed no damage after freeze-thaw cycling. Damage was assessed visually (scaling and spalling) and by identification of internal cracks with micro X-ray computed tomography (MXCT). **Figure 32** shows the relative dynamic modulus of elasticity for the control, PVA-g-PEG, and AEA test groups. The PVA-g-PEG modified samples performed as well or better than the AEA modified samples. **Figure 33** provides similar results for durability factor and length change.

The air void system parameters can be found in **Table 5**. The PVA-g-PEG samples entrain minimal air, less than 3% in the hardened state, and have a spacing factor greater than 300 μm. Based on the air content and spacing factor, poor performance in freeze-thaw testing would be expected. Taken with the results seen in paste, there is preliminary evidence to suggests that PVA-g-PEG enhances freeze-thaw resistance without the requirements of a traditional air void system. It is hypothesized that the IRI activity

of PVA-g-PEG results in lower hydraulic and crystallization pressures during cyclic freezing and thawing.

TABLE 4: Mix composition use for freeze-thaw testing of PVA-g-PEG.

Material (per cubic yard)	Test Group		
	Control	PVA-g-PEG	AEA
Cement (Type I/II) (lb.)	521	521	521
Fine aggregate (lb.)	1011	1011	1011
Coarse aggregate (lb.)	2040	2040	2040
Water/cement ratio (%)	50	50	50
PVA-g-PEG/cement ratio (%)	0	0.066	0
Air entraining agent (mL/220 lb cement)	0	0	15

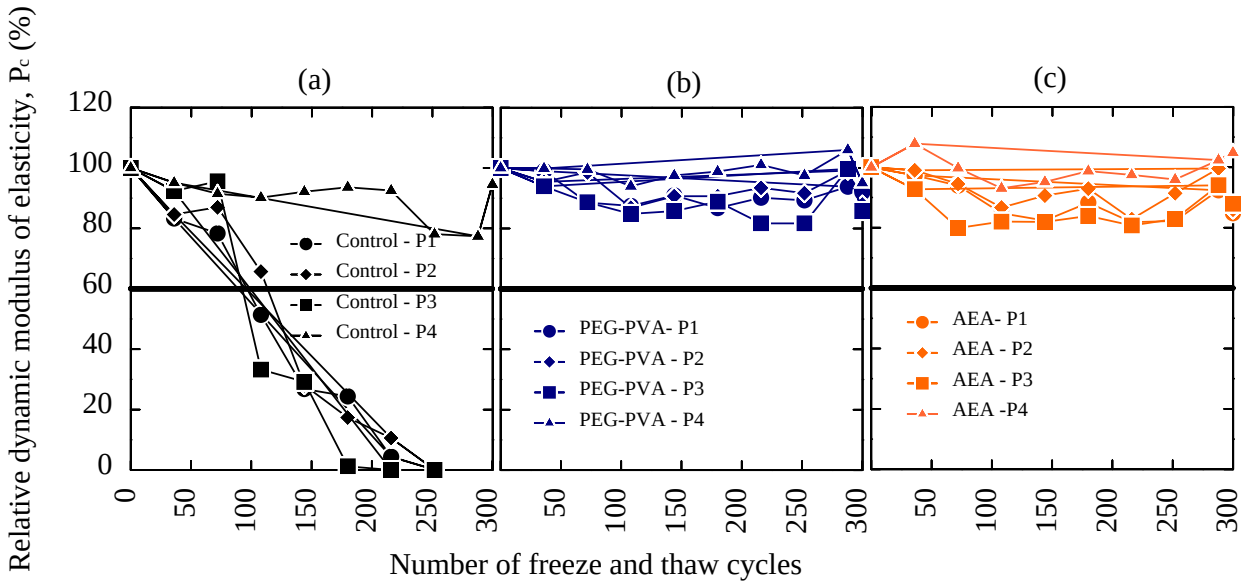

FIGURE 32: The relative dynamic modulus of elasticity (P_c) for each test group studied. For each test group, samples P1-P3 were exposed to cyclic freeze-thaw temperature while P4 was kept at ambient temperature. (a) Control, (b) 0.066 wt% PVA-g-PEG (PEG-PVA), (c) Air entraining agent addition (AEA). The line at P_c equal to 60% represents failure.

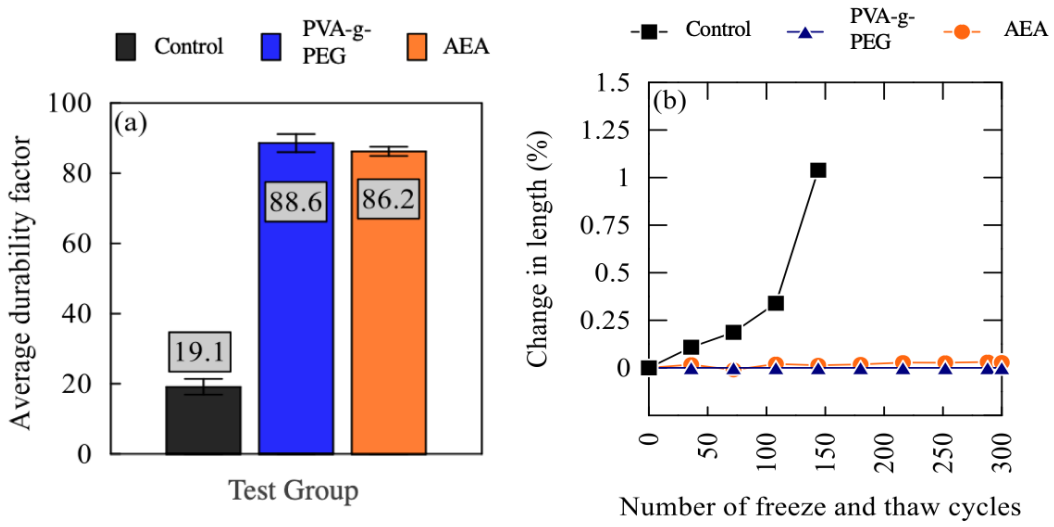

FIGURE 33: (a) Average durability factor for each test group. Error bars indicate the standard deviation for n=3. (b) Average length change (%) for each test group up to 300 freeze-thaw cycles. Average is for n=3 samples per test group.

TABLE 5: Air void parameters of control, PVA-g-PVA, and AEA concrete specimen.

	Test Group		
	Control	PVA-g-PEG	AEA
Fresh state air content (%)	2.1	4.2	7.0
Hardened state air content (%)	3.8	2.7	5.9
Spacing factor (μm)	1061	392	218

Plans for Implementation

The implementation plan describes the major tasks required to incorporate biomimetic antifreeze molecules (BAMs) into commercial applications, i.e., acting as a concrete additive for infrastructure.

1. There will be two (2) public disclosures of invention through the means of peer-reviewed publications within the first 12 months of project completion. A preliminary patent application has been filed with the US Patent Office. Conversion to a full patent application will be completed by Fall 2020.
2. A partnership for advanced testing and demonstration activities is being established with the Department of Defense Cold Regions Research and Engineering Laboratory. Advanced experiments on concrete formulations with different cement types, different types and amounts of supplementary cementitious materials, different water-to-cement ratios, and different polymers that also exhibit ice recrystallization inhibition are being designed. For example, new polymers

have been identified by the research team that will decrease the cost of the current BAM technology >10-fold. Prior to larger scale implementation and prototype trials outside of the laboratory, confirmation that the molecules are effective with each of the different concrete mixture formulations is essential.

3. Once the invention is refined and patent accepted, the facilitation of non-disclosure agreements (NDAs) with interested industry partners will commence. It is anticipated that a chemical admixture would be introduced to the marketplace within the next five (5) years.

Conclusions

The initial hypothesis stated that the biomimetic antifreeze molecules would serve well as novel deicing salt alternatives. However, it was found through this IDEA project that the antifreeze molecules would not effectively melt ice once it has formed nor would there be any additional synergistic benefit to using the molecules in tandem with traditional deicers.

Contrastingly, the initial hypothesis that biomimetic antifreeze molecules would prevent freeze-thaw damage in cement paste and concrete proved correct. The results of this IDEA concept provide the foundational work for biomimetic antifreeze molecules (BAMs) as an alternative to traditional air entraining agents for freeze-thaw resistance in concrete. The results of freeze-thaw testing clearly show that BAM modified cement paste and concrete are freeze-thaw resistant. The freeze-thaw resistance occurs with minimal air entrainment in concrete, <3% air content, and almost no air in paste (<1% air).

The results from this foundation project are particularly revolutionary in that the project team has identified a class of molecules that inhibit frost damage in concrete through a completely novel different mechanism never before discovered. Therefore, BAMs represent a new class of admixture technologies that has the potential to supplant conventional air-entraining admixture technology that has remained a common staple in the cement and concrete industry for >70 years.

Glossary and References

(1) Cwirzen, Andrzej, and Vesa Penttala. 2005. "Aggregate–Cement Paste Transition Zone Properties Affecting the Salt–Frost Damage of High-Performance Concretes." *Cement and Concrete Research* 35 (4): 671–79. https://doi.org/10.1016/j.cemconres.2004.06.009.

(2) M.J. Setzer, R. Auberg, and H.J. Keck. 2002. PRO 24: International RILEM Workshop on Frost Resistance of Concrete-From Nano-Structure and Pore Solution to Macroscopic Behaviour and Testing (Vol. 24). RILEM publications.

(3) Flatt, Robert J., Francesco Caruso, Asel Maria Aguilar Sanchez, and George W. Scherer. 2014. "Chemo-Mechanics of Salt Damage in Stone." *Nature Communications* 5 (1): 4823. https://doi.org/10.1038/ncomms5823.

(4) Scherer, George W. 2004. "Stress from Crystallization of Salt." *Cement and Concrete Research* 34 (9): 1613–24. https://doi.org/10.1016/j.cemconres.2003.12.034.

(5) Valenza, John J., and George W. Scherer. 2007. "A Review of Salt Scaling: II. Mechanisms." *Cement and Concrete Research* 37 (7): 1022–34. https://doi.org/10.1016/j.cemconres.2007.03.003.

(6) Scherer, George W., and John. J. Valenza. 2005. "Mechanisms of Frost Damage." *Materials Science of Concrete* 7: 209–46.

(7) American Highway Users Alliance. 2014. On Heels of Polar Vortex, Several Snow Falls, American Highway Users Alliance Releases New Data Highlighting Importance and Benefits of Safe Winter Road Operations [Press release]. Retrieved from http://www.highways.org/2014/01/winter-roads-release/

(8) G.H. Koch, M.P.H. Brongers, and N.G. Thompson. 2003. Corrosion Costs and Preventive Strategies in the United States. NACE International Report FHWA-RD-31-156. Retrieved from the TRIS and ITRD database.

(9) V.R. Kelly, S.E. Findlay, W.H. Schlesinger, K. Menking, and A.M. Chatrchyan. 2010. Road salt: Moving toward the solution. The Cary Institute of Ecosystem Studies, NY.

(10) Kelting, Daniel L, and Corey L Laxson. n.d. "Review of Effects and Costs of Road De-Icing with Recommendations for Winter Road Management in the Adirondack Park," 84.

(11) Claisse, Peter A. 2016. "Chapter 21 - Concrete Mix Design." In *Civil Engineering Materials*, edited by Peter A. Claisse, 201–17. Boston: Butterworth-Heinemann. https://doi.org/10.1016/B978-0-08-100275-9.00021-8.

(12) Chen, Xudong, Shengxing Wu, and Jikai Zhou. 2013. "Influence of Porosity on Compressive and Tensile Strength of Cement Mortar." *Construction and Building Materials* 40 (March): 869–74. https://doi.org/10.1016/j.conbuildmat.2012.11.072.

(13) Wong, H.S., A.M. Pappas, R.W. Zimmerman, and N.R. Buenfeld. 2011. “Effect of Entrained Air Voids on the Microstructure and Mass Transport Properties of Concrete.” *Cement and Concrete Research* 41 (10): 1067–77. https://doi.org/10.1016/j.cemconres.2011.06.013.

(14) “Concrete.” 2011. In *Building Materials in Civil Engineering*, 81–423. Elsevier. https://doi.org/10.1533/9781845699567.81.

(15) Li, Wenting, Mohammad Pour-Ghaz, Javier Castro, and Jason Weiss. 2012. “Water Absorption and Critical Degree of Saturation Relating to Freeze-Thaw Damage in Concrete Pavement Joints.” *Journal of Materials in Civil Engineering* 24 (3): 299–307. https://doi.org/10.1061/(ASCE)MT.1943-5533.0000383

(16) Davies, Peter L. 2014. “Ice-Binding Proteins: A Remarkable Diversity of Structures for Stopping and Starting Ice Growth.” *Trends in Biochemical Sciences* 39 (11): 548–55. https://doi.org/10.1016/j.tibs.2014.09.005.

(17) Voets, I. K. 2017. “From Ice-Binding Proteins to Bio-Inspired Antifreeze Materials.” *Soft Matter* 13 (28): 4808–23. https://doi.org/10.1039/C6SM02867E.

(18) Delesky, Elizabeth, Shane Frazier, Jaqueline Wallat, Kendra Bannister, Chelsea Heveran, and Wil Srubar. 2019. “Ice-Binding Protein from Shewanella Frigidimarinas Inhibits Ice Crystal Growth in Highly Alkaline Solutions.” *Polymers* 11 (2): 299. https://doi.org/10.3390/polym11020299.

(19) Ebbesen, Morten F., David H. Schaffert, Michael L. Crowley, David Oupický, and Kenneth A. Howard. 2013. “Synthesis of Click-Reactive HPMA Copolymers Using RAFT Polymerization for Drug Delivery Applications.” *Journal of Polymer Science Part A: Polymer Chemistry* 51 (23): 5091–99. https://doi.org/10.1002/pola.26941.

(20) Knight, Charles A., John Hallett, and A.L. DeVries. 1988. “Solute Effects on Ice Recrystallization: An Assessment Technique.” *Cryobiology* 25 (1): 55–60. https://doi.org/10.1016/0011-2240(88)90020-X.

(21) Mitchell, Daniel E., and Matthew I. Gibson. 2015. “Latent Ice Recrystallization Inhibition Activity in Nonantifreeze Proteins: Ca^{2+} -Activated Plant Lectins and Cation-Activated Antimicrobial Peptides.” *Biomacromolecules* 16 (10): 3411–16. https://doi.org/10.1021/acs.biomac.5b01118.

(22) Congdon, Thomas, Rebecca Notman, and Matthew I. Gibson. 2013. “Antifreeze (Glyco)Protein Mimetic Behavior of Poly(Vinyl Alcohol): Detailed Structure Ice Recrystallization Inhibition Activity Study.” *Biomacromolecules* 14 (5): 1578–86. https://doi.org/10.1021/bm400217j.

(23) Chaytor, J. L., J. M. Tokarew, L. K. Wu, M. Leclere, R. Y. Tam, C. J. Capicciotti, L. Guolla, et al. 2012. “Inhibiting Ice Recrystallization and Optimization of Cell Viability after Cryopreservation.” *Glycobiology* 22 (1): 123–33. https://doi.org/10.1093/glycob/cwr115.

(24) Kato, T. 2002. “Self-Assembly of Phase-Segregated Liquid Crystal Structures.” *Science* 295 (5564): 2414–18. https://doi.org/10.1126/science.1070967.

(25) Lock, Lye Lin, Michelle LaComb, Kelly Schwarz, Andrew G. Cheetham, Yi-an Lin, Pengcheng Zhang, and Honggang Cui. 2013. “Self-Assembly of Natural and Synthetic Drug Amphiphiles into Discrete Supramolecular Nanostructures.” *Faraday Discussions* 166: 285. https://doi.org/10.1039/c3fd00099k.

(26) Shi, Xianming, Laura Fay, Chase Gallaway, Kevin Volkening, Tongyan Pan, Andrew Creighton, Collins Lawlor, Yajun Liu, and Tuan Anh Nguyen. n.d. “Evaluation of Alternate Anti-Icing and Deicing Compounds Using Sodium Chloride and Magnesium Chloride as Baseline Deicers,” 294.

(27) Darwin, David, Frank G de Noyelles, and Carl E Locke. n.d. “HANDBOOK OF TEST METHODS FOR EVALUATING CHEMICAL DEICERS,” 290.

(28) Gerbino-Bevins, B. M., C. Y. Tuan, and M. Mattison. 2012. “Evaluation of Ice-Melting Capacities of Deicing Chemicals.” *Journal of Testing and Evaluation* 40 (6): 104460. https://doi.org/10.1520/JTE104460.

(29) Chatterji, S. 2003. “Freezing of Air-Entrained Cement-Based Materials and Specific Actions of Air-Entraining Agents.” *Cement and Concrete Composites* 25 (7): 759–65. https://doi.org/10.1016/S0958-9465(02)00099-9.

(30) C09 Committee. n.d. “Practice for Making and Curing Concrete Test Specimens in the Laboratory.” ASTM International. Accessed November 6, 2018a. https://doi.org/10.1520/C0192_C0192M-16A

(31) C01 Committee. n.d. “Specification for Mixing Rooms, Moist Cabinets, Moist Rooms, and Water Storage Tanks Used in the Testing of Hydraulic Cements and Concretes.” ASTM International. Accessed November 6, 2019. https://doi.org/10.1520/C0511-19.

(32) C09 Committee n.d. “Test Method for Resistance of Concrete to Rapid Freezing and Thawing.” ASTM International. Accessed November 6, 2018b. https://doi.org/10.1520/C0666_C0666M-15.

Appendix: Research Results

Sidebar Info

Program Steering Committee: NCHRP IDEA Program Committee December 2019
Title: Biomimetic Antifreeze Molecules: A Novel Solution to Deicing Salts and Air-Entraining Admixtures

Project Number: 204
Start Date: January 1, 2018 Completion Date: December 31, 2019

Product Category:

Principal Investigator: Wil V. Srubar III, Assistant Professor
E-Mail: wsrubar@colorado.edu
Phone: 303-492-2621

TITLE:

Biomimetic Antifreeze Molecules for Transportation Applications

SUBHEAD:

Biomimetic antifreeze molecules were evaluated as frost-prevention alternatives to surface-applied deicing salts and air-entraining admixtures in cement paste and concrete.

WHAT WAS THE NEED? Answer the following questions in 550–650 words.

For 100 years, the practice of using salt (*i.e.*, NaCl, $MgCl_2$) to depress the freezing point of water to improve the safety of vehicular traffic on roadways has remained virtually unchanged. A major drawback of deicing salt application is chloride-induced corrosion of steel and premature material failure in reinforced concrete. Similarly, for 70 years, the use of air entraining agents (AEAs) has remained unchanged. While AEAs inhibit freeze-thaw damage, entrained air is well known to decrease compressive strength and exacerbate other transport-related deterioration mechanisms (e.g., chloride-induced corrosion) by increasing the overall permeability of concrete.

WHAT WAS OUR GOAL?

The goal of this project was to design, synthesize, and test a class of biomimetic antifreeze molecules with behavior similar to natural antifreeze proteins found in fish, plants, insects, and bacteria. The molecules were evaluated for their effectiveness in (1) preventing or slowing ice formation and growth on roadway and bridge surfaces and (2) preventing frost damage in cement paste and concrete as an alternative to air entraining agents.

WHAT DID WE DO?

A series of biomimetic antifreeze molecules (BAMs), both polymeric and small molecule, were evaluated for ice recrystallization inhibition (IRI) and freezing point depression activity. Candidates that were IRI active, non-cytotoxic, and readily soluble in water were evaluated for their performance as deicing solutions and additives in concrete for freeze-thaw resistance.

WHAT WAS THE OUTCOME?

This project found that biomimetic antifreeze molecules would not effectively melt ice once it has formed nor would there be any additional synergistic benefit to using the molecules in tandem with conventional deicing salts, thereby limiting their effectiveness as a surface-applied alternative to traditional deicers. However, primary outcome of this research is the identification of a class of molecules that inhibit frost damage in concrete through a completely novel different mechanism never before discovered. Therefore, BAMs represent a new class of admixture technologies that has the potential to supplant conventional air-entraining admixture technology that has remained a common staple in the cement and concrete industry for >70 years.

WHAT IS THE BENEFIT?

This project discovered a new class of polymeric additives that can provide freeze-thaw resistance in cement paste and concrete without dependence on an entrained air void system. This new biomimetic approach provides several key advantages over traditional air entraining agents (AEAs), including (1) retention of compressive strength by minimizing entrained air and (2) reduced overall permeability, which subsequently leads to (3) increased long-term durability in chloride-laden environments. In summary, this work lays the scientific foundation for future research and development related to biomimetic antifreeze admixtures for use in concrete infrastructure prone to freeze-thaw deterioration.

LEARN MORE

For more information, please contact:

wsrubar@colorado.edu

IMAGES

Attachment 1. Final project presentation.